

MULTIOBJECTIVE OUTPUT FEEDBACK
via LMI OPTIMIZATION and QUARTER-CAR
ACTIVE SUSPENSION SYSTEM

Aslı SOYİÇ

Master of Science Thesis

Electrical and Electronics Engineering Program

December – 2009

JÜRİ VE ENSTİTÜ ONAYI

Aşlı Soyıç' in “**Doğrusal Matris Eşitsizlik Tabanlı Otomatik Kontrol ve Çeyrek Araç Modeli Aktif Süspansiyon Sistemine Uygulanması**” başlıklı **Elektrik–Elektronik Mühendisliği** Anabilim Dalındaki, Yüksek Lisans Tezi 24.11.2009 tarihinde, aşağıdaki jüri tarafından Anadolu Üniversitesi Lisansüstü Eğitim Öğretim ve Sınav Yönetmeliğinin ilgili maddeleri uyarınca değerlendirilerek kabul edilmiştir.

	Adı – Soyadı	İmza
Üye (Tez Danışmanı)	: Prof. Dr. HÜSEYİN AKÇAY
Üye	: Doç. Dr. AYDIN AYBAR
Üye	: Doç. Dr. YUSUF OYSAL

Anadolu Üniversitesi Fen Bilimleri Enstitüsü Yönetim Kurulu'nun
tarikh ve sayılı kararıyla onaylanmıştır.

Enstitü Müdürü

ÖZET

Yüksek Lisans Tezi

DOĞRUSAL MATRİS EŞİTSİZLİK TABANLI OTOMATİK KONTROL VE ÇEYREK ARAÇ MODELİ AKTİF SÜSPANSİYON SİSTEMİNE UYGULANMASI

Aslı SOYİÇ

Anadolu Üniversitesi

Fen Bilimleri Enstitüsü

Elektrik-Elektronik Mühendisliği Anabilim Dalı

Danışman : Prof. Dr. Hüseyin AKÇAY

2009, 50 sayfa

Bu tezde, doğrusal matris eşitsizlik tabanlı otomatik kontrol yaklaşımı ve bu yaklaşımın bir uygulaması olarak düşey ivme ölçümlü çeyrek araç modeli aktif süspansiyon sistemi tasarımı çalışılmıştır. Tasarım amaçları H_∞ performansı, H_2 performansı, zaman bölgesi kısıtları ve kapalı çevrim kutup alanındaki kısıtların bir karışımıdır. Tasarımı gerçekleştirebilmek için iki serbestlik dereceli çeyrek araç modelinin matematiksel ifadesi kullanılmış ve sistem beyaz gürültü yol girdisine göre tanımlanmıştır. Doğrusal matris eşitsizlik yaklaşımı ile geri beslemeli kontrolcü tasarımı yapılması amaçlanmıştır. Bu kontrolcünün süspansiyon ve tekerlek deformasyonunu istenilen değerlerde tutarken, yolcu konforunu sağlamak amacıyla düşey ivmeyi mümkün olduğu kadar küçültebilmesi gerekmektedir. MATLAB simülasyonları kullanılarak, aktif süspansiyon ve pasif süspansiyon sistemleri karşılaştırılması yapılmıştır. Önerilen yaklaşım, kısıtları verilen değerlerde tutarken mümkün olan en iyi yol konforunu sağlamaktadır.

Anahtar Kelimeler : Doğrusal Matris Eşitsizlikleri; Otomatik Kontrol; Çeyrek

Araç Modeli; Aktif Süspansiyon

ABSTRACT

Master of Science Thesis

MULTIOBJECTIVE OUTPUT FEEDBACK CONTROL via LMI OPTIMIZATION and QUARTER-CAR ACTIVE SUSPENSION SYSTEM

Ash SOYIÇ

Anadolu University

Graduate School of Sciences

Electrical and Electronics Engineering Program

Supervisor : Prof. Dr. Hüseyin AKÇAY

2009, 50 pages

In this thesis, the linear matrix inequality approach to multiobjective synthesis of linear output-feedback controllers is investigated. Design objectives are a mixture of the H_∞ performance, H_2 performance, the time-domain constraints, and the constraints on the closed-loop pole locations. As an application of the LMI approach, the quarter-car model active suspension system design with vertical acceleration measurement is studied. Two degree of freedom quarter-car model is defined and parametrized to the white noise velocity road inputs. Multiobjective output feedback controller is designed in order to minimize the rms vertical acceleration for achieving better ride comfort while keeping the tire deflection rms gain and the suspension travel rms response below some given bounds. MATLAB simulations of active and passive suspension systems are compared. The proposed approach achieves best possible ride comfort while keeping the constrained variables within the given bounds.

Keywords : Linear Matrix Inequalities; Active Suspension; Quarter-Car Model;

Multiobjective Control

Acknowledgements

I would like to express my sincere appreciation to my thesis supervisor, Prof. Dr. Hüseyin AKÇAY for his supervision throughout this study.

I thank to my family for their patience and support through this study.

Aslı SOYİÇ

December 2009

Contents

ÖZET	i
ABSTRACT	ii
ACKNOWLEDGEMENTS	iii
CONTENTS	iv
LIST OF FIGURE	vi
LIST OF TABLES	viii
1 INTRODUCTION	1
1.1 Scope of the Work.....	3
2 MULTIOBJECTIVE OUTPUT FEEDBACK CONTROL via LMI OPTIMIZATION	4
2.1 Linear Matrix Inequality - LMI.....	4
2.1.1 Problem Statement and the motivation.....	4
2.1.2 The LMI formulation of the design specifications.....	6
2.1.3 The LMI approach to multiobjective synthesis.....	9
2.1.4 The LMI's for full order synthesis	11
2.2 Quarter-Car Model	13
2.2.1 Application to the active suspension design problem	16
3 RESULTS of the LMI APPROACH on the QUARTER-CAR VEHICLE MODEL	18
3.1 Design Example with the Tire Deflection Rms Gain Constraint	18
3.2 Design Example with the Tire Deflection Rms Gain Constraint and the Rms Suspension Travel.....	23
3.3 Design Example with Constraints on the Rms Tire Deflection and the Rms Suspension Travel.....	28
4 CONCLUSIONS	32
4.1 Future of Work	32

BIBLIOGRAPHY	34
Appendix A	38
Appendix B	41
Appendix C	46

List of Figures

2.1 The feedback configuration.....	5
2.2 2 DOF quarter car model.....	14
3.1 The vertical acceleration, the suspension travel and the tire deflection frequency responses with $\lambda = 0.1$, $\mu = 1$ and $C_t = 50$ Ns/m; (—) passive suspension, (-.-) active suspension	19
3.2 The rms values and the tire deflection rms gain of the vehicle subjected to white noise velocity input as a function of C_t with $\lambda = 0.1$ and $\mu = 1$; (—) passive suspension, (-.-) active suspension	20
3.3 The vertical acceleration, the suspension travel and the tire deflection frequency responses with $\lambda = 0.1$, $\mu = 2$ and $C_t = 50$ Ns/m; (—) passive suspension, (-.-) active suspension	21
3.4 The rms values and the tire deflection rms gain of the vehicle subjected to white noise velocity input as a function of C_t with $\lambda = 0.1$ and $\mu = 2$; (—) passive suspension, (-.-) active suspension	22
3.5 The rms values and the tire deflection rms gain of the vehicle subjected to white noise velocity input as a function of C_t with $\alpha = 1$ and $\mu = 1$; (—) passive suspension, (-.-) active suspension	24
3.6 The vertical acceleration, the suspension travel and the tire deflection frequency responses with $\alpha = 1$, $\mu = 2$ and $C_t = 50$ Ns/m; (—) passive suspension, (-.-) active suspension	25
3.7 The rms values and the tire deflection rms gain of the vehicle subjected to white noise velocity input as a function of C_t with $\alpha = 1$ and $\mu = 2$; (—) passive suspension, (-.-) active suspension	26
3.8 The rms values and the tire deflection rms gain of the vehicle subjected to white noise velocity input as a function of C_t with $\alpha = 2$ and $\mu = 1$; (—) passive suspension, (-.-) active suspension	27

3.9	The vertical acceleration, the suspension travel and the tire deflection frequency responses with $\alpha = 1$, $\mu = 1$ and $C_t = 50$ Ns/m; (—) passive suspension, (-.-) active suspension	29
3.10	The rms values and the tire deflection rms gain of the vehicle subjected to white noise velocity input as a function of C_t with $\alpha = 1$ and $\mu = 1$; (—) passive suspension, (-.-) active suspension	30

List of Tables

2.1	The system parameters and values of the quarter-car model	15
3.1	The rms values of z_k , $k = 1,2,3$, and the tire deflection rms gain table of passive and active suspension systems with $\lambda = 0.1$, $\mu = 1$ and $C_t = 50$ Ns/m	19
3.2	The rms values of z_k , $k = 1,2,3$, and the tire deflection rms gain table of passive and active suspension systems with $\lambda = 0.1$, $\mu = 2$ and $C_t = 50$ Ns/m	20
3.3	The rms values of z_k , $k = 1,2,3$, and the tire deflection rms gain table of passive and active suspension systems with $\alpha = 1$, $\mu = 1$ and $C_t = 50$ Ns/m	23
3.4	The rms values of z_k , $k = 1,2,3$, and the tire deflection rms gain table of passive and active suspension systems with $\alpha = 1$, $\mu = 2$ and $C_t = 50$ Ns/m	25
3.5	The rms values of z_k , $k = 1,2,3$, and the tire deflection rms gain table of passive and active suspension systems with $\alpha = 2$, $\mu = 1$ and $C_t = 50$ Ns/m	27
3.6	The rms values of z_k , $k = 1,2,3$, and the tire deflection rms gain table of passive and active suspension systems with $\alpha = 1$, $\mu = 1$ and $C_t = 50$ Ns/m	28
3.7	The rms values of z_k , $k = 1,2,3$, and the tire deflection rms gain table of passive and active suspension systems with $\alpha = 1$, $\mu = 2$ and $C_t = 50$ Ns/m	31
3.8	The rms values of z_k , $k = 1,2,3$, and the tire deflection rms gain table of passive and active suspension systems with $\alpha = 2$, $\mu = 1$ and $C_t = 50$ Ns/m	31

CHAPTER 1

INTRODUCTION

The suspension systems serve a dual purpose – contributing to the car's handling and braking for good active safety and driving pleasure, and keeping vehicle occupants comfortable and reasonably well isolated from road noise, bumps and vibrations. Automotive suspension systems are divided into three categories; passive suspension systems, semi-active suspension systems and active suspension systems according to their ability to add or extract energy.

It is well known that compromise between ride comfort and handling performance has to be made to design passive suspension of a vehicle. To overcome this problem, many researchers have proposed to use active suspension systems.

An active suspension system, has the capability to adjust itself continuously to changing road conditions. It artificially extends the design parameters of the system by constantly monitoring and adjusting itself, thereby changing its character on an ongoing basis.

Also, active suspensions may consume large amounts of energy in providing the control force and therefore in the design procedure for the active suspension the power limitations of actuators should also be considered as an important factor. In any vehicle suspension system, there are a variety of performance parameters which need to be optimized. Among them, three main performance requirements for advanced vehicle suspensions include isolating passengers from vibration and shock arising from road roughness (ride comfort), suppressing the hop of the wheels so as to maintain firm and uninterrupted contact of wheels to road (good handling), keeping suspension strokes within an allowable maximum (structural constraint) and restricting the active force due to the limited power provided by the vehicle engine [5,28]. These requirements are conflicting, and in order to manage the trade-offs between conflicting performance requirements, many active suspension control approaches are

proposed on various control techniques such as LQG (Linear Quadratic Gaussian) control, adaptive control, nonlinear control, H_∞ or H_2 control and also LMI approach (e.g.[1, 2, 3, 4, 5, 6, 16, 17, 27, 28]).

In this thesis, the LMI approach is applied to the active suspension system design problem. For getting a general view of control problems, a brief information about control problems and methods are given below.

The mathematical formulation of control problems, based on mathematical models of physical systems, is intrinsically complex, the fundamental ideas in control theory are simple enough and very intuitive. These key ideas can be found in nature, in the evolution and the behaviour of living beings [26].

There are three fundamental concepts in control theory; the first one is that of feedback. The second key concept in control theory is that of need for fluctuations. And the third very important concept in control theory is that of optimization. The last one, optimization, is a very well established branch of mathematics, whose goal is to find the values for variables in order to maximize the profit or to minimize the costs subject to some constraints [26, 11].

The problem of designing controllers that satisfy both the robust stability and some performance criteria is called robust control. The H_∞ control theory is one of the cornerstones of modern control theory. It was developed to solve such problems with very strong practical implications. The widely accepted modern technique for solving robust control problems now is to reduce them to linear matrix inequalities (LMIs) and the LMI techniques are commonly examined in most researches and books (e.g.[9, 10, 11, 13, 14, 18]).

The LMIs and the LMI techniques have emerged as powerful design tools in areas ranging from control engineering to system identification and structural design. Three factors make LMI techniques appealing:

- a variety of design specifications and constraints can be expressed as LMIs
- once formulated in terms of LMIs, a problem can be solved exactly by efficient convex optimization algorithms (the “LMI solvers”)

- while most problems with multiple constraints or objectives lack analytical solutions in terms of matrix equations, they often remain tractable in the LMI framework. This makes LMI-based design a valuable alternative to classical “analytical” methods [2, 11].

In active suspension system design, system requirements, mentioned above, only the first one, which provides ride comfort to passengers, requires a minimum while the others have to keep related states within the given bounds. These requirements are in fact hard constraints in time-domain and related to safety. Then the active suspension control problem can be considered as a disturbance attenuation problem with time-domain hard constraints [4, 5]. According to these informations, in this thesis, the LMI optimization is suggested to apply to the active suspension design problem.

1.1 Scope of the Work

In this thesis, multiobjective output-feedback control with LMI synthesis of a quarter-car active suspension system is studied. The design of a output-feedback controller that provides a better ride comfort and respects all constraints of active suspension system is aimed. The content of this thesis is organized as follows:

First, in Chapter 2, the LMIs are studied. Formulations, variables and feasibility of the synthesis to the control problems are reviewed. In this chapter, also the quarter-car model of a vehicle is presented. The LMI synthesis is applied to the quarter-car model.

In Chapter 3, the LMI control procedure reviewed in Chapter 2 is applied to the quarter-car active suspension design problem for three cases. Firstly, the problem is stated and the variables are defined for the three cases. A parametric design study for different cases of the parameters is performed.

CHAPTER 2

MULTIOBJECTIVE OUTPUT FEEDBACK CONTROL via LMI OPTIMIZATION

2.1 Linear Matrix Inequality – LMI

The history of LMIs in the analysis of dynamical systems goes back more than 100 years ago. The history has begun in about 1890, when Lyapunov published his seminal work. He showed that the differential equation

$$\frac{d}{dt}x(t) = Ax(t) \quad (2.1)$$

is stable if and only if there exists a positive definite matrix P satisfying

$$A^T P + PA < 0. \quad (2.2)$$

The requirement $A^T P + PA < 0$ is what we nowadays call a Lyapunov inequality on P is a special form of an LMI [13, 22].

2.1.1 Problem statement and the motivation

The LMIs have emerged as powerful formulation and design techniques for a variety of linear-control problems. Since solving the LMIs is a convex optimization problem, such formulations offer a numerically tractable means of attacking problems that lack an analytical solution [1].

In this thesis, multiobjective output-feedback synthesis for multi-input/multi-output (MIMO) linear time invariant (LTI) systems is studied. The feedback configuration is as follows ;

$$\begin{aligned} \dot{x} &= Ax + B_1 w + B_2 u \\ z_\infty &= C_\infty x + D_{\infty 1} w + D_{\infty 2} u \\ z_2 &= C_2 x + D_{21} w + D_{22} u \\ y &= Cx + D_y u \end{aligned} \quad (2.3)$$

where $u \in \mathcal{R}^{n_u}$ is the control input, w is the exogenous input, $y \in \mathcal{R}^{n_y}$ is the measured output, z_∞ and z_2 forms the outputs channels. \mathcal{R} denotes the real

numbers, n_u and n_y indicate the size of u and y respectively. The output channel z_∞ is associated with the H_∞ performance while the channel z_2 is associated with the H_2 performance.

The dynamical output-feedback controller shown in 2.1 and denoted by K satisfies $u = Ky$. Its realization is given by state-space ;

$$\begin{aligned}\dot{\xi} &= A_K \xi + B_K y \\ u &= C_K \xi + D_K y\end{aligned}\quad (2.4)$$

where A_K, B_K, C_K, D_K are the state-space parameters.

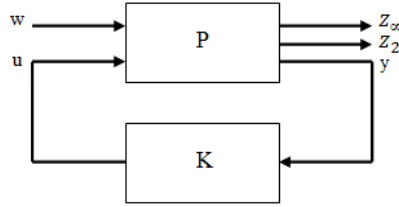


Figure 2.1 : The feedback configuration

The closed-loop equations have the following form :

$$\begin{aligned}\dot{x}_{cl} &= A_{cl} x_{cl} + B_{cl} w \\ z_\infty &= C_{cl\infty} x_{cl} + D_{cl\infty} w \\ z_2 &= C_{cl2} x_{cl} + D_{cl2} w\end{aligned}\quad (2.5)$$

where

$$\begin{aligned}A_{cl} &= \begin{pmatrix} A + B_2 \Gamma D_K C & B_2 \Gamma C_K \\ B_K C + B_K D_y \Gamma D_K C & A_K + B_K D_y \Gamma C_K \end{pmatrix}, & B_{cl} &= \begin{pmatrix} B_1 \\ 0 \end{pmatrix}, \\ C_{cl\infty} &= (C_\infty + D_{\infty 2} \Gamma D_K C \quad D_{\infty 1} \Gamma C_K), & D_{cl\infty} &= D_{\infty 2}, \\ C_{cl2} &= (C_{cl2} + D_{22} \Gamma D_K C \quad D_{21} \Gamma C_K), & D_{cl2} &= D_{22}, \\ \Gamma &= (1 - D_K D_y)^{-1} \quad \text{and} \quad x_{cl} = [x \quad \xi]^T.\end{aligned}\quad (2.6)$$

The closed-loop transfer function from w_j to z_j is denoted by $T_j(s)$ and w_j and z_j are the specified input and output signals.

2.1.2 The LMI formulation of the design specifications

All the LMI characterizations are listed below. A_{cl} is the closed-loop state matrix and x_{cl} is the closed-loop state vector in equation (2.6).

Since the closed-loop system must be internally stable, it must admit a quadratic Lyapunov function [1] :

$$V_{cl} = x_{cl}^T P x_{cl}, \quad P > 0 \quad (2.7)$$

such that

$$A_{cl}^T P + P A_{cl} < 0. \quad (2.8)$$

The LMI consists of expressing each control specification or objectives as an additional constraint on admissible closed-loop Lyapunov functions satisfying (2.7) and (2.8) [1,8,6].

- **H_∞ Performance**

T_∞ is the closed-loop transfer matrix from the input w to the output channel z_∞ . Let $\|T_\infty\|_\infty$ denote the H_∞ norm of T_∞ that is, its largest gain across frequency in the singular value. The H_∞ norm of T_∞ is also defined as,

$$\|T_\infty\|_\infty = \max_w \frac{\|z_\infty\|_2}{\|w\|_2}.$$

The H_∞ norm measures the system input-output gain for finite energy or finite rms input signals. For more information, see [11].

The H_∞ nominal performance can be formulated as follows. The constraint $\|T_\infty\|_\infty < \gamma$, for $\gamma > 0$ can be interpreted as a disturbance rejection performance [1,11]. The closed-loop rms gain from w to z_∞ does not exceed γ if and only if there exists a symmetric matrix P_∞ such that

$$\begin{pmatrix} A_{cl}P_{\infty} + P_{\infty}A_{cl}^T & B_{cl} & P_{\infty}C_{cl\infty}^T \\ B_{cl}^T & -I & D_{cl\infty}^T \\ C_{cl\infty}P_{\infty} & D_{cl\infty} & -\gamma I \end{pmatrix} < 0, \quad (2.9)$$

$$P_{\infty} > 0. \quad (2.10)$$

The closed-loop matrices A_{cl} , B_{cl} , $C_{cl\infty}$ and $D_{cl\infty}$ are defined by equations (2.5) and (2.6).

- **H_2 Performance**

T_2 is the closed-loop transfer function from the input w to the output channel z_2 , is defined in equation (2.5). The H_2 norm of $\|T_2\|_2$ is defined by

$$\|T_2\|_2^2 = \frac{1}{2\pi} \int_{-\infty}^{\infty} \text{Tr}(T_2^H(jw)T_2(jw))dw$$

and corresponds to the asymptotic variance of the output z_2 when the system is driven by the white noise input w . It is well-known that is norm can be computed as

$$\|T_2\|_2^2 = \inf \{ \text{Trace}(C_{cl2}P_2C_{cl2}^T) : A_{cl}P_2 + P_2A_{cl}^T + B_{cl}B_{cl}^T < 0 \}$$

where $D_{cl2} = 0$ [2].

The *inf* denotes *infimum* and in mathematics, particularly set theory, the *infimum* of a subset of some set is the greatest element that is less than or equal to all elements of the subset.

Lets define the H_2 nominal performance. The H_2 norm of the closed-loop transfer function from w to z_2 does not exceed ν , for $\nu > 0$ if and only if $D_{cl2} = 0$ and there exists two symmetric matrices P_2 and Q such that [2,11]

$$\begin{pmatrix} A_{cl}P_2 + P_2A_{cl}^T & B_{cl} \\ B_{cl}^T & -I \end{pmatrix} < 0, \quad (2.11)$$

$$\begin{pmatrix} Q & C_{cl2}P_2 \\ P_2C_{cl2}^T & P_2 \end{pmatrix} > 0, \quad (2.12)$$

$$\text{Trace}(Q) < v^2. \quad (2.13)$$

The closed-loop matrices A_{cl} , B_{cl} , C_{cl2} and D_{cl2} are defined by equations (2.5) and (2.6).

Note that the trace of $n \times n$ square matrix W is defined by

$$\text{Tr}(W) \equiv \sum_{i=1}^n w_{ii},$$

it is the sum of diagonal elements. For more information, see [30].

- **Generalized H_2 Performance**

The generalized H_2 norm is defined by

$$\|T_j\|_g = \sup \{ \|z_j(T)\| : x_{cl}(0) = 0, \text{ for } T \geq 0, \int_0^T \|w_j(t)\|^2 dt \leq 1 \}. \quad (2.14)$$

It measures the peak amplitude of the output signal $z_j(t)$ over all unit-energy inputs $w_j(t)$ [1].

Suppose that there exists a symmetric matrix P_2 satisfying

$$\begin{pmatrix} A_{cl}P_2 + P_2A_{cl}^T & B_{cl} \\ B_{cl}^T & -I \end{pmatrix} < 0, \quad (2.15)$$

$$\begin{pmatrix} P_2 & C_{cl2}^T \\ C_{cl2} & \delta I \end{pmatrix} > 0, \quad D_{cl2} = 0. \quad (2.16)$$

The first inequality ensures that $(d/dt)V(x_{cl}(t)) - w_j(t)^T w_j(t) \ll 0$ and the second inequality implies that $(1/\delta)C_{cl2}^T C_{cl2} < P_2$ and thus $z_j(T)^T z_j(T) \leq \delta V(x_{cl}(T))$. Combining these two inequalities leads to

$$z_j(T)^T z_j(T) \ll \delta \int_0^T w_j(t)^T w_j(t) dt$$

for all $T \geq 0$, so $\|T_j\|_g^2 < \delta$ [1].

- **Pole Placement**

The closed-loop poles lie in the LMI region

$$D = \{z \in \mathbf{C} : L + Rz + R^T z^T < 0\}$$

with $L = L^T = [l_{ij}]_{1 \leq i, j \leq m}$ and $R = [\mu_{ij}]_{1 \leq i, j \leq m}$ if and only if there exists a symmetric matrix P_{pol} satisfying

$$[l_{ij}P_{pol} + \mu_{ij}A_{cl}P_{pol} + \mu_{ij}P_{pol}A_{cl}^T]_{1 \leq i, j \leq m} < 0, \quad (2.17)$$

$$P_{pol} > 0. \quad (2.18)$$

To recover convexity, it must be required that all specifications are enforced by a single closed-loop Lyapunov function [3, 8, 6]. This amounts to imposing the constraint

$$P = P_\infty = P_2 = P_{pol}. \quad (2.19)$$

2.1.3 The LMI approach to multiobjective synthesis

The main goal is to compute a single LTI controller K that

1. internally stabilizes the closed-loop and
2. meets certain specifications on a particular set of channels [1].

n is the number of states of the plant (size of A) and k is the order of controller.

Partition P and P^{-1} as,

$$P = \begin{pmatrix} Y & N \\ N^T & * \end{pmatrix}, \quad P^{-1} = \begin{pmatrix} X & M \\ M^T & * \end{pmatrix} \quad (2.20)$$

where X and Y are $n \times n$ and symmetric real matrices. * replaces blocks that are readily inferred by symmetry.

From $PP^{-1} = I$,

$$P\Pi_1 = \Pi_2 \quad \text{with} \quad \Pi_1 := \begin{pmatrix} X & I \\ M^T & 0 \end{pmatrix} \quad (2.21)$$

$$\Pi_2 := \begin{pmatrix} I & Y \\ 0 & N^T \end{pmatrix}. \quad (2.22)$$

The motivation for the transformation of controller parameters lies in the following identities derived from (2.6), (2.21) and (2.22) after a short calculation [1, 29] :

$$\begin{aligned} \Pi_1^T P A_{cl} \Pi_1 &= \Pi_2^T A_{cl} \Pi_1 = \begin{pmatrix} AX + B_2 \tilde{C} & A + B_2(1 - D_K D_y)^{-1} \tilde{D} C \\ \tilde{A} & YA + \tilde{B} C \end{pmatrix} \\ \Pi_1^T P B_{cl} &= \Pi_2^T B_{cl} = \begin{pmatrix} B_1 \\ Y B_1 \end{pmatrix} \\ C_{cl\infty} \Pi_1 &= (C_\infty X + D_{\infty 1} \tilde{C} \quad C_\infty + D_{\infty 1}(1 - D_K D_y)^{-1} D_K C) \\ C_{cl2} \Pi_1 &= (C_2 X + D_{21} \tilde{C} \quad C_2 + D_{21}(1 - D_K D_y)^{-1} D_K C) \\ \Pi_1^T P \Pi_1 &= \Pi_1^T \Pi_2 = \begin{pmatrix} X & I \\ I & Y \end{pmatrix} \end{aligned} \quad (2.23)$$

where the change of controller variables in equation (2.23) \tilde{A} , \tilde{B} , \tilde{C} and \tilde{D} as follows :

$$\begin{cases} \tilde{A} = N A_K M^T + Y(A + B_2 \Gamma D_K C)X + N B_K (I + D_y \Gamma D_K) C X \\ \quad + (Y^T B_2 \Gamma + N B_K D_y \Gamma) C_K M^T \\ \tilde{B} = Y^T B_2 \Gamma D_K + N B_K D_y \Gamma D_K + N B_K \\ \tilde{C} = \Gamma D_K C X + \Gamma C_K M^T \\ \tilde{D} = D_K \end{cases} \quad (2.24)$$

Note that the new variables \tilde{A} , \tilde{B} , \tilde{C} in equations (2.24) have dimensions $n \times n$, $n \times n_u$, and $n_y \times n$ respectively. If M and N have full row rank and \tilde{A} , \tilde{B} , \tilde{C} , \tilde{D} , X , and Y are given, the controller matrices A_K , B_K , C_K and D_K that satisfy (2.4) can always be computed. If M and N matrices are square and invertible then controller matrices A_K , B_K , C_K and D_K are unique. For full order design M and N can always be assumed that have full row rank. Hence, the variables A_K , B_K , C_K and D_K can be replaced by \tilde{A} , \tilde{B} , \tilde{C} and \tilde{D} without loss of generality [1, 2].

In the light of these identities synthesis of LMI's can be derived from analysis results of Section (2.1.2) with a suitable transformation.

At first, a detailed proof for the generalized H_2 problem is provided. Fix $\delta > 0$ and suppose that equations (2.15), (2.16) and (2.19) hold for some $P > 0$ and some controller with realization (A_K, B_K, C_K, D_K) . That can be assumed without loss of generality, this controller is of order at least n (size of A) and M and N in equation (2.20) have full row rank. From equation (2.21), since P is nonsingular, Π_1 has full column rank [1]. If a suitable transformation with $diag(\Pi_1, I)$ is performed to inequalities in (2.15) and (2.16), take the forms :

$$\begin{pmatrix} \Pi_1^T A_{cl}^T P \Pi_1 + \Pi_1^T P A_{cl} \Pi_1 & \Pi_1^T P B_{cl} \\ B_{cl}^T P \Pi_1 & -I \end{pmatrix} < 0, \quad (2.25)$$

$$\begin{pmatrix} \Pi_1^T P \Pi_1 & \Pi_1^T C_{cl2}^T \\ C_{cl2} \Pi_1 & \delta I \end{pmatrix} > 0. \quad (2.26)$$

Now replace the equations from equation (2.23) in inequalities (2.25) and (2.26), then inequalities take forms :

$$\begin{pmatrix} \Lambda_{11} & \tilde{A}^T + A + B_2 \Gamma \tilde{D} C & B_1 \\ \tilde{A} + A^T + (B_2 \Gamma \tilde{D} C)^T & \Lambda_{22} & Y B_1 \\ B_1^T & B_1^T & -I \end{pmatrix} < 0, \quad (2.27)$$

$$\begin{pmatrix} X & I & (C_2 X + D_{22} \tilde{C})^T \\ I & Y & (C_2 + D_{22} \Gamma D_K C)^T \\ C_2 X + D_{22} \tilde{C} & C_2 + D_{22} \Gamma D_K C & \delta I \end{pmatrix} > 0, \quad (2.28)$$

with

$$\Lambda_{11} = X A^T + A X + B_2 \tilde{C} + \tilde{C}^T B_2^T,$$

$$\Lambda_{22} = (Y A + \tilde{B} C)^T + Y A + \tilde{B} C.$$

These inequalities are clearly affine in \tilde{A} , \tilde{B} , \tilde{C} , \tilde{D} , X , and Y . Thus, the solvability of these LMI's is *necessary* for the existence of a stabilizing controller rendering the inequality $\|T\|_g^2 < \delta$ [1].

2.1.4 The LMI's for full order synthesis

The LMI formulation for each particular specification is outlined this section. For example, our design problem has an H_∞ constraint and also an H_2 constraint.

H_∞ Synthesis

In the H_∞ synthesis, the analysis LMI's (2.9) and (2.10) are transformed with Π_1 and $diag(\Pi_1, I, I)$. Then, inequalities take form :

$$\begin{pmatrix} \Sigma_{11} & \Sigma_{12} & B_1 & (C_\infty X + D_{12} \tilde{C})^T \\ * & \Sigma_{22} & YB_1 & (C_\infty + D_{12} \Gamma D_K C)^T \\ * & * & -\gamma I & D_{11}^T \\ * & * & * & -\gamma I \end{pmatrix} < 0 \quad (2.29)$$

where

$$\Sigma_{11} = XA^T + AX + B_2 \tilde{C} + \tilde{C}^T B_2^T,$$

$$\Sigma_{12} = \tilde{A}^T + A + B_2 \Gamma \tilde{D} C,$$

$$\Sigma_{22} = (YA + \tilde{B}C)^T + (YA + \tilde{B}C)$$

and * denotes symmetric elements of the matrix. Since γ enters linearly, it can be directly minimized by the LMI optimization to find the smallest achievable H_∞ norm [1].

Generalized H₂ Synthesis

In the generalized H_2 synthesis, the analysis LMI's (2.11) – (2.13) are transformed with $diag(\Pi_1, I)$ for the standart H_2 problem. Inequalities obtained as shown in (2.30) – (2.32) :

$$\begin{pmatrix} \Sigma_{11} & \tilde{A}^T + A + B_2 \Gamma \tilde{D} C & B_1 \\ * & (YA + \tilde{B}C)^T + (YA + \tilde{B}C) & YB_1 \\ * & * & -I \end{pmatrix} < 0, \quad (2.30)$$

$$\begin{pmatrix} X & I & (C_2 X + D_{22} \tilde{C})^T \\ I & Y & (C_2 + D_{22} \Gamma D_K C)^T \\ (C_2 X + D_{22} \tilde{C}) & (C_2 + D_{22} \Gamma D_K C) & Q \end{pmatrix} > 0, \quad (2.31)$$

$$Trace(Q) < \nu \quad (2.32)$$

where Σ_{11} denotes to $XA^T + AX + B_2 \tilde{C} + \tilde{C}^T B_2^T$.

Regional Pole Placement

The matrix $diag(\Pi_1, \dots, \Pi_1)$ transforms inequality (2.17) to the LMI :

$$\left(\begin{array}{c} l_{jk} \left(\begin{array}{cc} X & I \\ I & Y \end{array} \right) + \mu_{jk} \left(\begin{array}{cc} AX + B_2 \tilde{C} & A + B_2 \tilde{D} C \\ & \tilde{A} \quad YA + \tilde{B} C \end{array} \right)^T \\ + \mu_{kj} \left(\begin{array}{cc} AX + B_2 \tilde{C} & A + B_2 \tilde{D} C \\ & \tilde{A} \quad YA + \tilde{B} C \end{array} \right) \end{array} \right)_{jk} < 0. \quad (2.33)$$

Also, since the requirement $P > 0$ is common to all analysis results in Section (2.1.2), the constraint

$$\left(\begin{array}{cc} X & I \\ I & Y \end{array} \right) > 0 \quad (2.34)$$

should always be included in the list of LMI's [1, 2, 11].

2.2 Quarter – Car Model

Performance requirements for advanced vehicle suspensions include;

1. isolating passengers from vibration and shock arising from road roughness (ride comfort),
2. suppressing the hop of the wheels so as to maintain firm and uninterrupted contact of wheels to road (good road holding),
3. keeping suspension strokes within an allowable maximum [4, 5].

In order to manage the trade-offs between conflicting performance requirements, many active suspension control approaches based on various control techniques such as LQG, adaptive control and nonlinear control have been proposed in the literature. A common point of these approaches is that all control requirements are weighted and formulated in a single objective function to be minimized in order to find an optimum controller [4, 5].

In designing an active suspension system, one needs to take the following aspects into consideration ;

- as an indicator of ride comfort, the sprung mass vertical acceleration should be made as small as possible.

- the suspension travel should be kept below, the maximum allowable suspension stroke to prevent excessive suspension bottoming, which can result in structural damage and deterioration of ride comfort.
- the dynamic tire load should not exceed the static ones, that is,

$$k_t(x_2 - w) + C_t(\dot{x}_2 - \dot{w}) < 9.8(m_s - m_u)$$

- to avoid actuator saturation, the active force should be bounded, i.e., for some $U > 0$, $u(t) \leq U$ for all t [3].

Thus designing control law for the suspension system is a multi-objective control problem.

Figure 2.2 shows a two degree of freedom (2 DOF) quarter-car model where m_s and m_u denotes the sprung and the unsprung masses respectively. The pair (k_s, C_s) is the so-called passive suspension; k_t stands for the tire stiffness and C_t denotes the tire damping. The parameter values, except C_t , chosen for this study are shown in Table 2.1 [3].

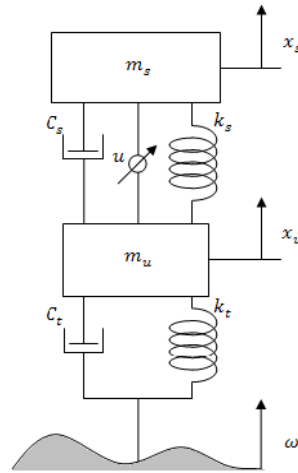


Figure 2.2 : 2 DOF quarter-car model

Equations of motion take the following form :

$$m_s \ddot{x}_s = -k_s(x_s - x_u) - C_s(\dot{x}_s - \dot{x}_u) - u$$

$$m_u \ddot{x}_u = k_s(x_s - x_u) + C_s(\dot{x}_s - \dot{x}_u) + u - k_t(x_u - w) - C_t(\dot{x}_u - \dot{w})$$

where x_s is the displacement of the sprung mass, x_u is the displacement of the unsprung mass and w is the road unevenness. To transform the equations of motion

of the quarter-car model into a state-space form, the following state variables are defined.

x_1 : suspension travel $x_s - x_u$

x_2 : tire deflection $x_u - w$

x_3 : sprung mass absolute velocity \dot{x}_s

x_4 : unsprung mass absolute velocity \dot{x}_u .

m_s	Sprung mass	240 kg
m_u	Unsprung mass	36 kg
C_s	Damping coefficient	980 Ns/m
k_s	Suspension stiffness	16,000 N/m
k_t	Tire stiffness	160,000 N/m

Table 2.1 : The system parameters and values of the quarter-car model

The output vector z consists of the vertical acceleration, the suspension travel, and the tire deflection.

$z_1 = \dot{x}_3$: vertical acceleration of the sprung mass,

$z_2 = x_1$: the suspension travel,

$z_3 = x_2$: the tire deflection.

All achievable rms responses of the quarter-car model are parametrized to the white noise velocity road inputs [3, 27]. We assume that the derivative of w denoted by V_i obeys the relation [27] :

$$V_i = \dot{w} = 2\pi n_0 \sqrt{\kappa v} \eta(t), \quad t \geq 0 \quad (2.36)$$

where $\eta(t)$ is a zero-mean white noise process with an autocovariance function $R_\eta(\tau) = \delta(\tau)$; κ and n_0 are the road roughness parameters; v is the vehicle forward velocity; and $\delta(t)$ is the unit impulse function [3]. For this study n_0 and κ assume the values 0.15708 cycles per meter and 0.76×10^5 respectively. The vehicle forward velocity is 20 m/s.

From equations (2.35) and (2.36) we obtain,

$$\begin{aligned} \dot{x} &= Ax + B_1 V_i + B_2 u \\ z &= C_z x + D_{zw} V_i + D_{zu} u \\ y &= Cx + D_y u \end{aligned} \quad (2.37)$$

where

$$A = \begin{pmatrix} 0 & 0 & 1 & -1 \\ 0 & 0 & 0 & 1 \\ -\frac{k_s}{m_s} & 0 & -\frac{c_s}{m_s} & \frac{c_s}{m_s} \\ \frac{k_s}{m_u} & -\frac{k_t}{m_u} & \frac{c_s}{m_u} & -\frac{(c_s+c_t)}{m_u} \end{pmatrix} \quad (2.38)$$

$$B_1 = \begin{pmatrix} 0 \\ -1 \\ 0 \\ \frac{c_t}{m_u} \end{pmatrix}, \quad B_2 = \begin{pmatrix} 0 \\ 0 \\ -\frac{1}{m_s} \\ \frac{1}{m_u} \end{pmatrix}, \quad (2.39)$$

$$C_z = \begin{pmatrix} -\frac{k_s}{m_s} & 0 & -\frac{c_s}{m_s} & \frac{c_s}{m_s} \\ 1 & 0 & 0 & 0 \\ 0 & 1 & 0 & 0 \end{pmatrix}, \quad D_{zw} = \begin{pmatrix} 0 \\ 0 \\ 0 \\ 0 \end{pmatrix}, \quad D_{zu} = \begin{pmatrix} -\frac{1}{m_s} \\ 0 \\ 0 \end{pmatrix}, \quad (2.40)$$

$$C = \begin{pmatrix} -\frac{k_s}{m_s} & 0 & -\frac{c_s}{m_s} & \frac{c_s}{m_s} \end{pmatrix}, \quad D_y = -\frac{1}{m_s}. \quad (2.41)$$

2.2.1 Application to the active suspension design problem

In this section, multiobjective output control via LMI optimization is applied to design active suspension system, based on a two degree of freedom quarter-car model studied in Section 2.2.

For application of the LMI control to the quarter-car model system, we must define z_∞ and z_2 outputs as in equation (2.3). Then, the quarter-car model in equation (2.37) takes the form :

$$\begin{aligned} \dot{x} &= Ax + B_1 V_i + B_2 u \\ z_\infty &= C_\infty x + D_{\infty 1} V_i + D_{\infty 2} u \\ z_2 &= C_2 x + D_{21} V_i + D_{22} u \\ y &= Cx + D_y u. \end{aligned} \quad (2.42)$$

In this thesis, the tire deflection is chosen as z_∞ output and, the vertical acceleration and the suspension travel are chosen as z_2 output. Thus,

$$C_\infty = (0 \ 1 \ 0 \ 0), \quad D_{\infty 1} = (0), \quad D_{\infty 2} = (0), \quad (2.43)$$

$$C_2 = \begin{pmatrix} -\frac{k_s}{m_s} & 0 & -\frac{c_s}{m_s} & \frac{c_s}{m_s} \\ 1 & 0 & 0 & 0 \end{pmatrix}, \quad D_{21} = \begin{pmatrix} 0 \\ 0 \end{pmatrix}, \quad D_{22} = \begin{pmatrix} -\frac{1}{m_s} \\ 0 \end{pmatrix}. \quad (2.44)$$

CHAPTER 3

RESULTS of the LMI APPROACH on the QUARTER-CAR VEHICLE MODEL

In this chapter, results, obtained from designing a controller for suspension system of a vehicle by using LMI control, are studied. The frequency response plots, the rms values plots and the rms values of both active and passive suspension systems are presented. The results for different parameters are compared to each other. So, we tried to get an outcome about solution of the problem. For getting all of these results, MATLAB LMI Control Toolbox [2] was used.

3.1 Design Example with Tire Deflection Rms Gain Constraint

The problem is: for given numbers $\gamma, \rho_1, \rho_2 > 0$, design an output feedback controller $u = K(s)y$ that satisfies $\|T_{z_3V_i}\|_\infty < \gamma$ and minimizes $\rho_1 \|T_{z_1V_i}\|_2^2 + \rho_2 \|T_{z_2V_i}\|_2^2$ [3].

The parameters γ, ρ_1 and ρ_2 of the multiobjective control problem are the design parameters. Let $G_{z_kV_i}$ denotes the open loop transfer function from V_i to the output variable z_k where $k = 1, 2, 3$. For some positive parameters λ and μ , the parameters are chosen as $\rho_1 = \|G_{z_1V_i}\|_2^{-1}$, $\rho_2 = \|G_{z_2V_i}\|_2^{-1}\lambda$ and $\gamma = \|G_{z_3V_i}\|_\infty\mu$. The parameters λ and μ control the trade-offs.

This problem is solved by the *hinfmix* command of MATLAB LMI Control Toolbox. A MATLAB code implementing the design is provided in *Appendix A*. Figure 3.1 shows the frequency responses of the active and passive suspension systems with parameters $\lambda = 0.1$, $\mu = 1$, and $C_t = 50$ Ns/m with the vertical acceleration and the suspension travel measurements. Table 3.1 shows the rms values of active and passive suspension systems.

	Passive Susp. System	Active Susp. System
The rms vertical acceleration	0.5337	0.4887
The rms suspension travel	0.0046	0.0045
The rms tire deflection	0.0017	0.0016
The tire deflection rms gain	0.0347	0.0304

Table 3.1 : The rms values of z_k , $k = 1,2,3$, and the tire deflection rms gain table of passive and active suspension systems with $\lambda = 0.1$, $\mu = 1$ and $C_t = 50$ Ns/m

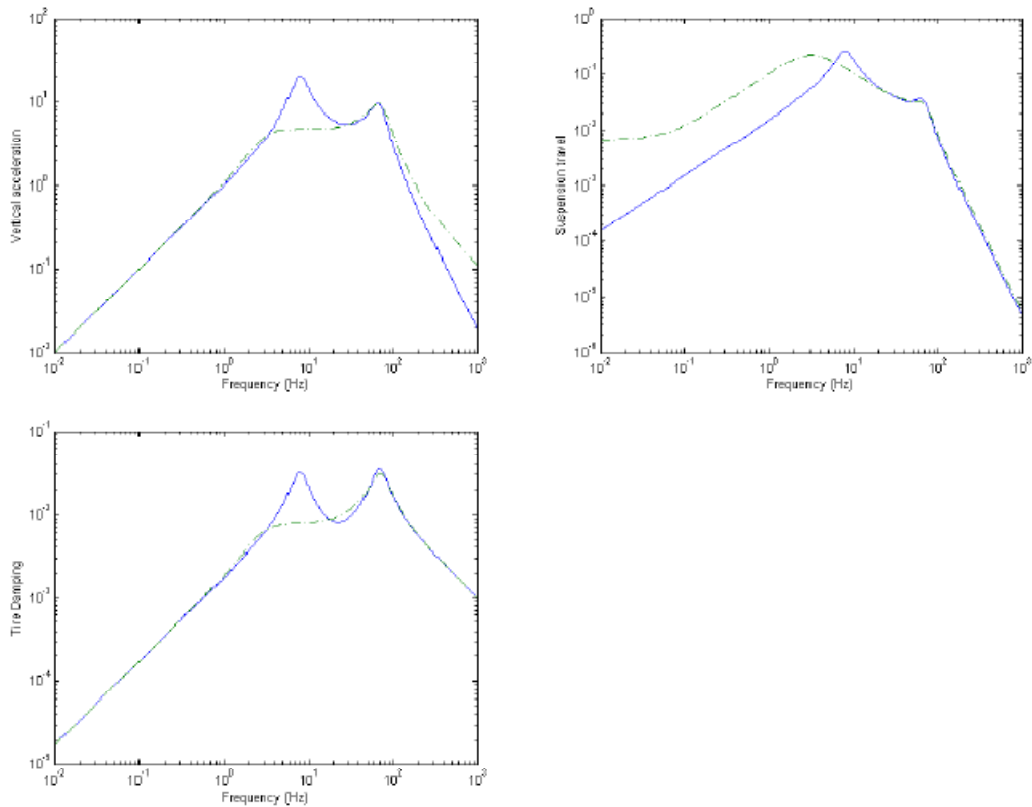


Figure 3.1 : The vertical acceleration, the suspension travel and the tire deflection frequency responses with $\lambda = 0.1$, $\mu = 1$ and $C_t = 50$ Ns/m; (—) passive suspension, (-.-) active suspension

The vertical acceleration-tire deflection and the suspension travel-tire deflection trade-offs are notable. The declining responses as functions of the tire damping indicate that the tire damping improves passive and active suspension performances [5]. Figure 3.2 shows the rms values of z_k , $k = 1,2,3$ and the tire deflection rms gain of the vehicle subjected to the white noise velocity input as a function of C_t with parameters $\lambda = 0.1$ and $\mu = 1$.

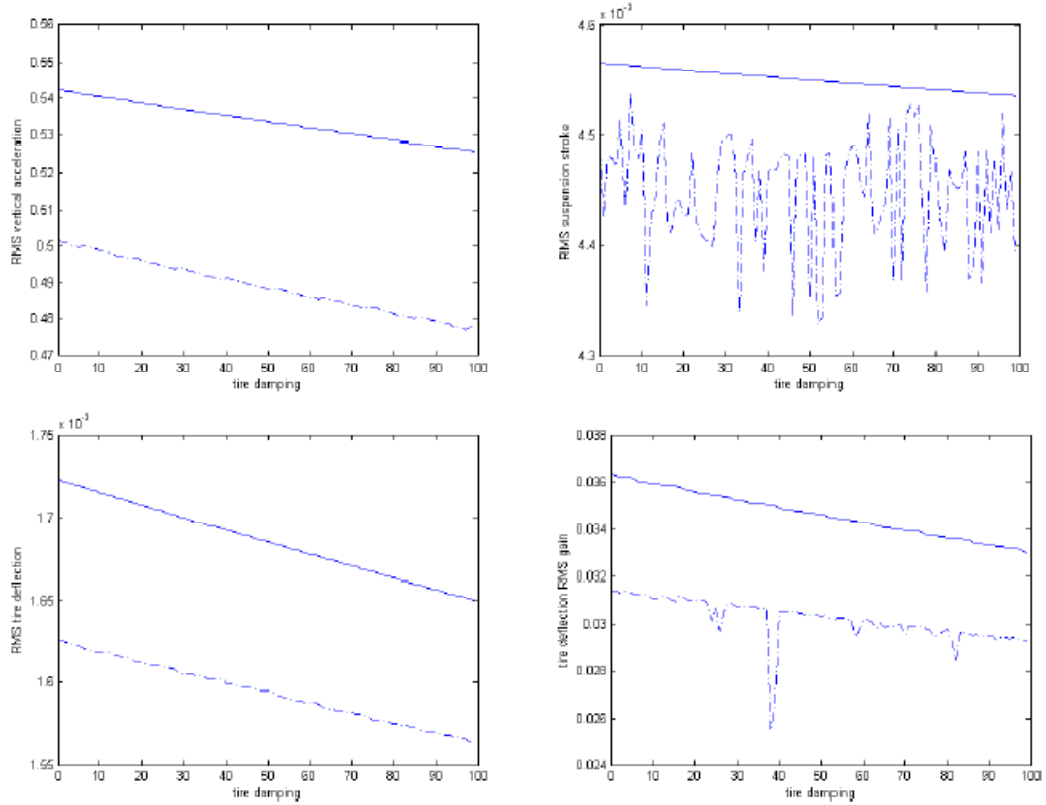


Figure 3.2 : The rms values and the tire deflection rms gain of the vehicle subjected to white noise velocity input as a function of C_t with $\lambda = 0.1$ and $\mu = 1$; (—) passive suspension, (-.-) active suspension

Now lets change parameters and again examine the results. For $\lambda = 0.1$ and $\mu = 2$, and no change in other parameters, the results are as shown in Figure 3.3.

	The Closed-Loop Rms Values
The rms vertical acceleration	0.3208
The rms suspension travel	0.0054
The rms tire deflection	0.0022
The tire deflection rms gain	0.0615

Table 3.2 : The rms values of z_k , $k = 1,2,3$, and the tire deflection rms gain table of passive and active suspension systems with $\lambda = 0.1$, $\mu = 2$ and $C_t = 50$ Ns/m

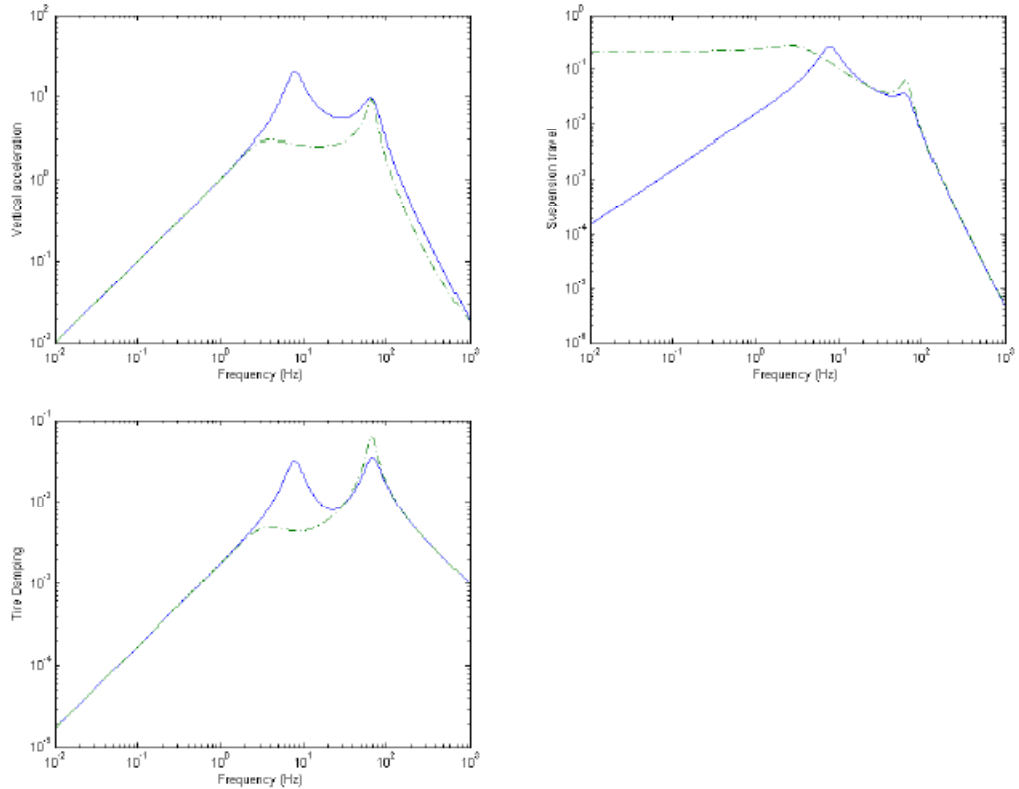


Figure 3.3 : The vertical acceleration, the suspension travel and the tire deflection frequency responses with $\lambda = 0.1$, $\mu = 2$ and $C_t = 50$ Ns/m; (—) passive suspension, (-.-) active suspension

From these bode plots and the rms values, we do not observe any improvement in the design. Because, when the vertical acceleration rms value decreased, the suspension travel and also the rms tire deflection rised. In bode plots, especially in the frequency range 4~8 Hertz where the human body is much sensitive to vibrations in the vertical direction, results are good. But, on the other hand, besides this interval, active system gives us worse and inconsistent results in comparison the passive system.

In Figure 3.4 the rms values as a function of the tire damping for a range between 0 and 100 Ns/m are plotted for $\lambda = 0.1$ and $\mu = 2$.

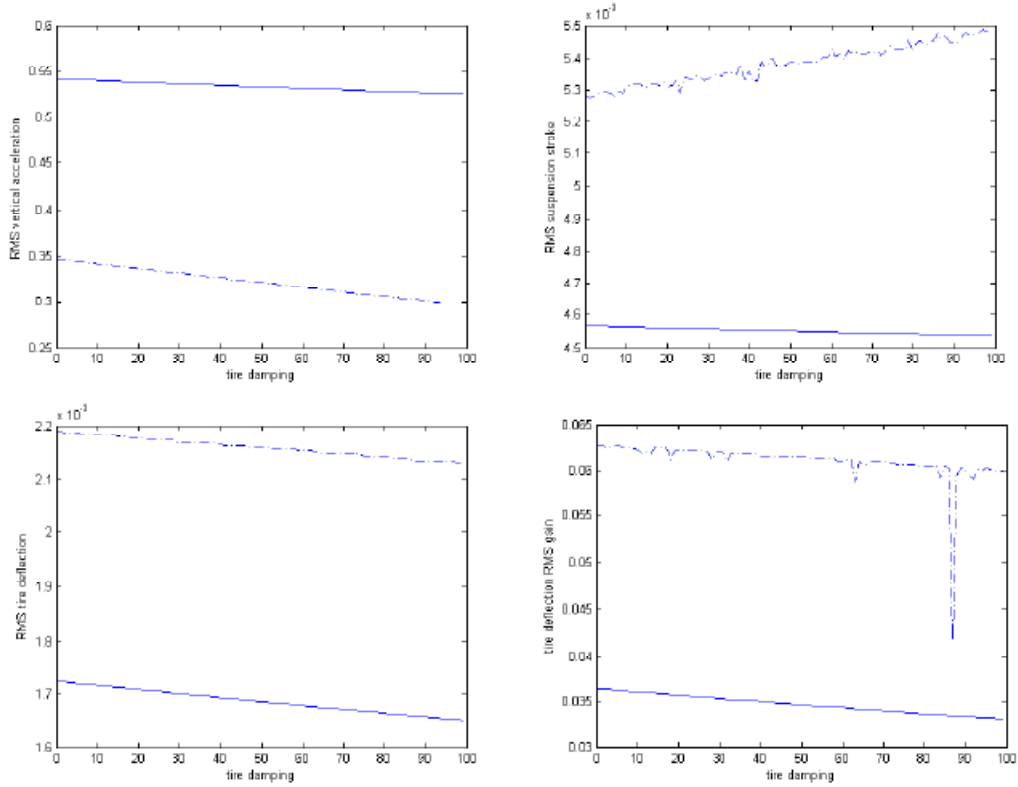


Figure 3.4 : The rms values and the tire deflection rms gain of the vehicle subjected to white noise velocity input as a function of C_t with $\lambda = 0.1$ and $\mu = 2$; (—) passive suspension, (-.-) active suspension

The results do not confirm our predictions about the active suspension design.

From the results, we conclude that when we increase value of the parameter μ , we also increase the limit of the constraint. Therefore, the tire damping rms gain is rised, and contingently suspension stroke rms value also is rised. But, on the other hand, the vertical acceleration falls down in accordance with them.

We examined whether it was possible to reduce the rms vertical acceleration without increasing the rms suspension travel and the rms tire deflection. In the next design ezample, our objective is to minimize the rms vertical acceleration while keeping the tire deflection rms gain and the suspension travel rms response below some given bounds.

3.2 Design Example with Tire Deflection Rms Gain Constraint and Rms Suspension Travel Constraint

Let's add another constraint to the design problem. New problem is: for given numbers $\gamma, \rho_1, \nu > 0$, design an output feedback controller $u = K(s)y$ that satisfies $\|T_{z_3 v_i}\|_\infty < \gamma$, $\|T_{z_2 v_i}\|_2 < \nu$ and minimizes $\rho_1 \|T_{z_1 v_i}\|_2^2$.

Now, a new parameter ν is introduced for the rms suspension travel constraint. We will use this new parameter in changing limit 2 – norm of the suspension travel of active suspension system and examine its effect on the design.

Lets choose values of $\nu = \|G_{z_2 v_i}\|_2 \alpha$ and $\gamma = \|G_{z_3 v_i}\|_\infty \mu$, where α and μ are scaling parameters that control the constraints. In addition to these choices, ρ_2 will be accepted 1. New parameter α is also 1 at first.

After all parameter values are determined, we get the rms values and plots. Firstly, Table 3.3 has the rms values of active suspension system obtained by running the MATLAB code given in *Appendix B*. In this table, we accepted $\alpha = 1$, $\mu = 1$ and $C_t = 50$ Ns/m.

	The Closed-Loop Rms Values
The rms vertical acceleration	0.4891
The rms suspension travel	0.0042
The rms tire deflection	0.0016
The tire deflection rms gain	0.0304

Table 3.3 : The rms values of z_k , $k = 1,2,3$, and the tire deflection rms gain table of passive and active suspension systems with $\alpha = 1$, $\mu = 1$ and $C_t = 50$ Ns/m

A comparison of the results in Table 3.3 with the result in the Table 3.1 shows that the second design problem improves the rms suspension travel value. On the other hand, the first design example yields 8.43% improvement on the rms vertical acceleration, as opposed to in the second design problem 8.36% improvement. They are very close to each other so that the difference between

them can be neglected. Figure 3.5 shows the rms value plots as C_t is varied from 0 to 100 Ns/m.

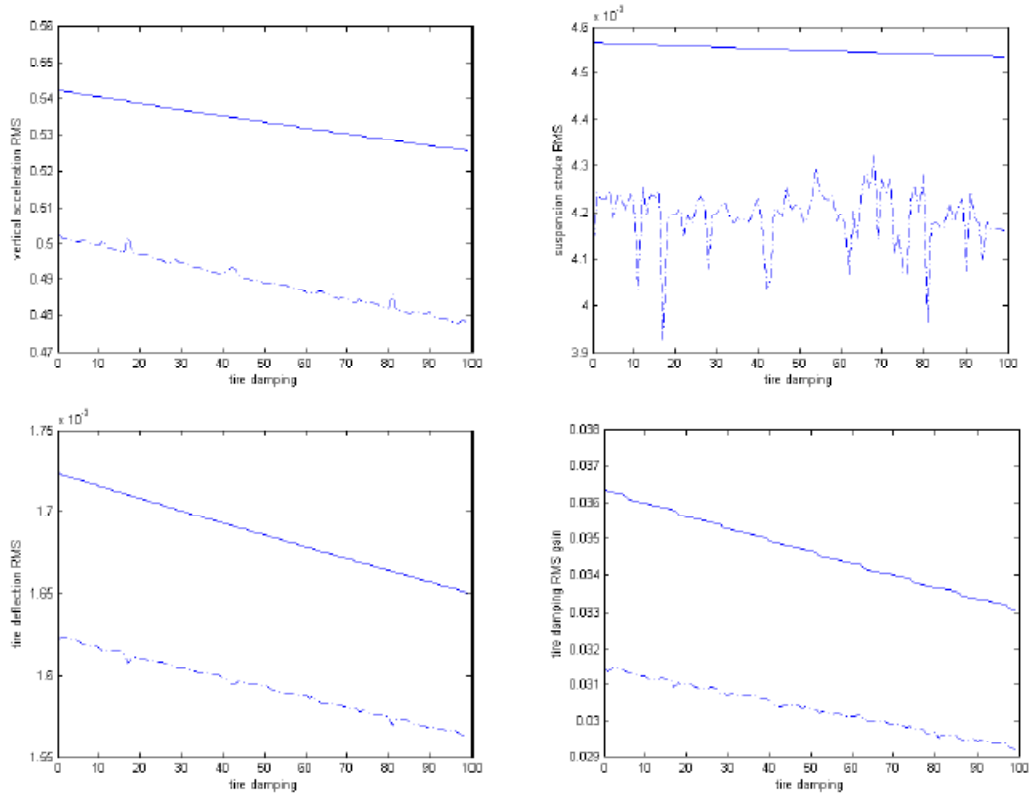


Figure 3.5 : The rms values and the tire deflection rms gain of the vehicle subjected to white noise velocity input as a function of C_t with $\alpha = 1$ and $\mu = 1$; (—) passive suspension, (-.-) active suspension

In Figure 3.6, the vertical acceleration, the suspension travel, and the tire deflection frequency responses of the active suspension system designed with parameters $\alpha = 1$, $\mu = 1$ and $C_t = 50$ Ns/m are plotted.

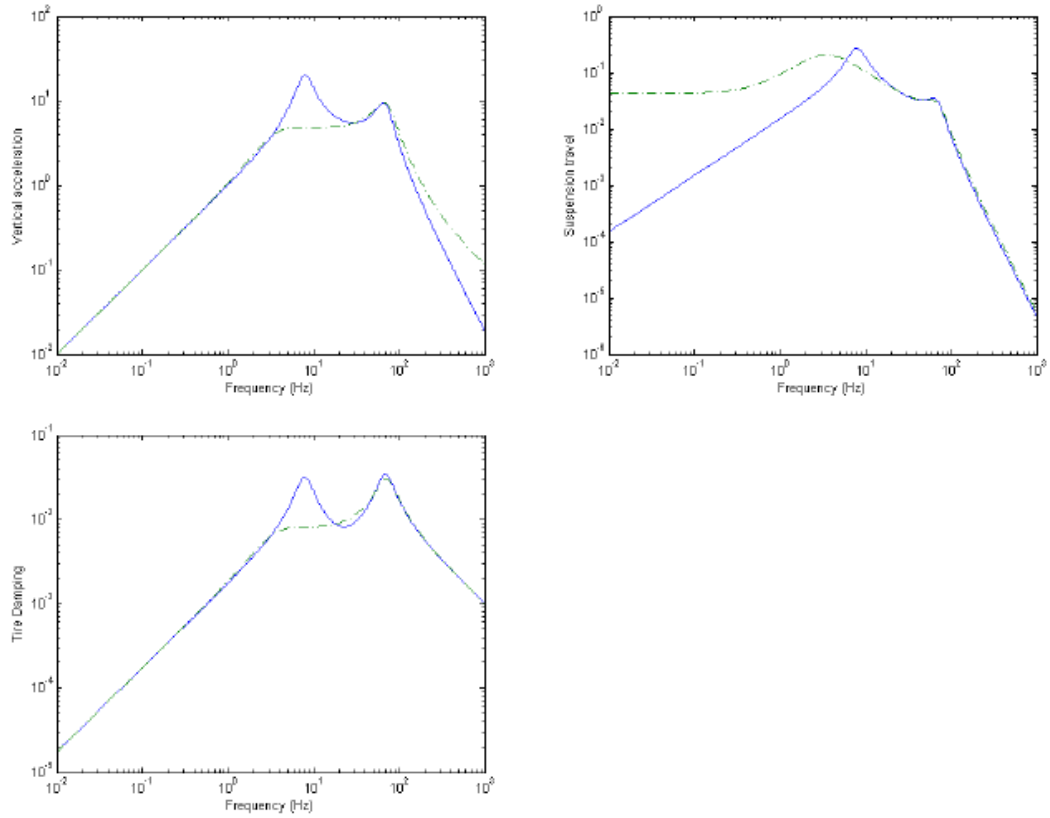


Figure 3.6 : The vertical acceleration, the suspension travel and the tire deflection frequency responses with $\alpha = 1$, $\mu = 1$ and $C_t = 50$ Ns/m; (—) passive suspension, (-.-) active suspension

Now, let us examine the changes in the suspension response when the upper bound on the rms tire deflection is changed. We set $\mu = 2$ and keep the remaining parameters value as before.

	The Closed-Loop Rms Values
The rms vertical acceleration	0.4019
The rms suspension travel	0.0044
The rms tire deflection	0.0018
The tire deflection rms gain	0.0428

Table 3.4 : The rms values of z_k , $k = 1,2,3$, and the tire deflection rms gain table of passive and active suspension systems with $\alpha = 1$, $\mu = 2$ and $C_t = 50$ Ns/m

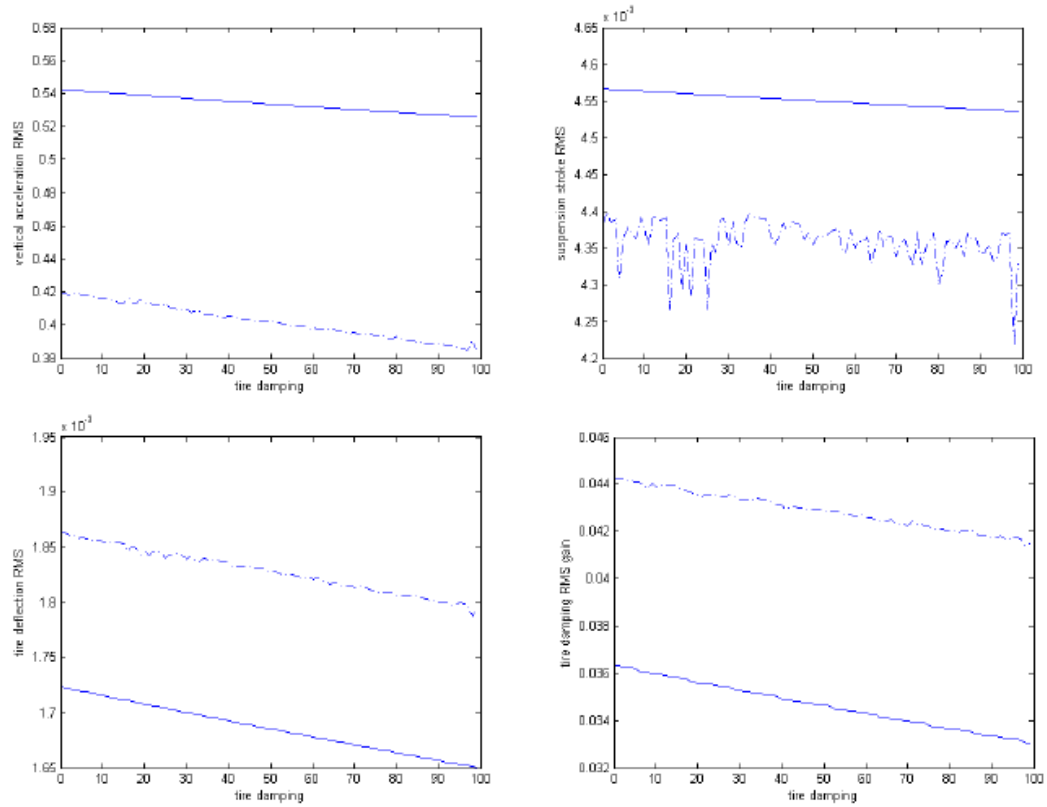


Figure 3.7 : The rms values and the tire deflection rms gain of the vehicle subjected to white noise velocity input as a function of C_t with $\alpha = 1$ and $\mu = 2$; (—) passive suspension, (-.-) active suspension

Until now, the upper bound on the rms tire deflection was changed and the effect of this change on the rms values of other outputs of interest and the frequency response were studied. In the first design example, for different values of μ , not only the rms tire deflection increased but also the rms suspension travel increased above their maximums. Then, in the second design example, we added a new constraint on the rms suspension travel, and μ is changed, the rms suspension travel was kept below the upper limit. Both the rms suspension travel and the rms tire deflection were below the given bounds and also the rms vertical acceleration was reduced. Figure 3.7 and Table 3.4 show us the rms suspension travel increased a little when the rms tire deflection increased. The MATLAB code is given in the *Appendix B* is used to solve the second design example.

How about effects of changes in the suspension travel constraint? What happened that the suspensiontravel constraint limit is increased with no other change in the problem? Now lets try to change the suspension travel limit with $\alpha = 2$ and look at how it effects the results. The results are shown in Table 3.5.

	The Closed-Loop Rms Values
The rms vertical acceleration	0.4881
The rms suspension travel	0.0056
The rms tire deflection	0.0016
The tire deflection rms gain	0.0304

Table 3.5 : The rms values of z_k , $k = 1,2,3$, and the tire deflection rms gain table of passive and active suspension systems with $\alpha = 2$, $\mu = 1$ and $C_t = 50$ Ns/m

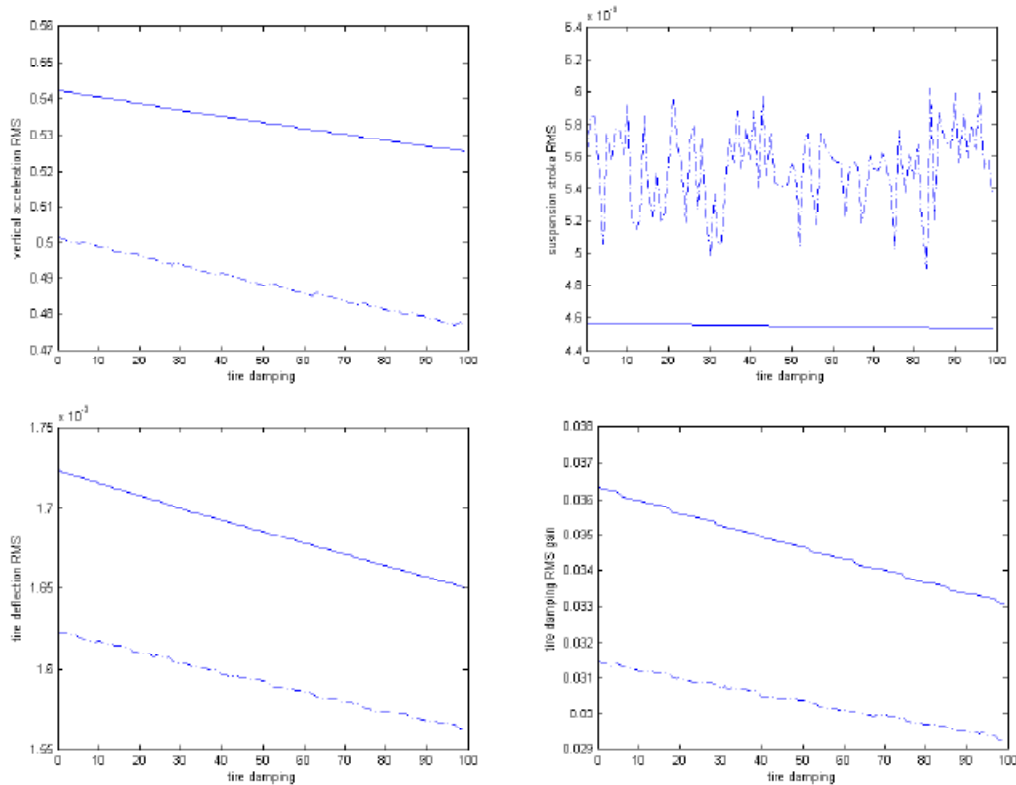


Figure 3.8 : The rms values and the tire deflection rms gain of the vehicle subjected to white noise velocity input as a function of C_t with $\alpha = 2$ and $\mu = 1$; (—) passive suspension, (-.-) active suspension

As it is obviously seen from the values on the Table 3.5 and Figure 3.8, changing only the rms suspension travel limit value is not enough to exceed the rms tire deflection upper bound. With this design, we can reduce the rms vertical acceleration without increasing the rms suspension travel and the rms tire deflection.

3.3 Design Example with Constraints on the Rms Tire Deflection and the Rms Suspension Travel

In this design example, the design problem has been simplified just a little. We have focused only on the rms vertical acceleration.

The new problem is: for given numbers $\gamma, \nu > 0$, design an output feedback controller $u = K(s)y$ that satisfies $\|T_{z_3 v_i}\|_\infty < \gamma$, $\|T_{z_2 v_i}\|_2 < \nu$ and minimizes $\|T_{z_1 v_i}\|_2^2$.

First of all, the design parameters must be chosen with vertical acceleration measurement. The all parameters are accepted as the previous design example except ρ_1 . The parameter ρ_1 equals to 1 in this design example. The results obtained by running the MATLAB code given in *Appendix C* for different parameter values.

We begin with parameters $\alpha = 1$ and $\mu = 1$. Figure 3.9 shows the frequency response of active and passive suspension systems with the constant tire damping $C_t = 50$. Table 3.6 has the active system rms values.

	The Closed-Loop Rms Values
The rms vertical acceleration	0.4898
The rms suspension travel	0.0042
The rms tire deflection	0.0016
The tire deflection rms gain	0.0303

Table 3.6 : The rms values of z_k , $k = 1,2,3$, and the tire deflection rms gain table of passive and active suspension systems with $\alpha = 1$, $\mu = 1$ and $C_t = 50$ Ns/m

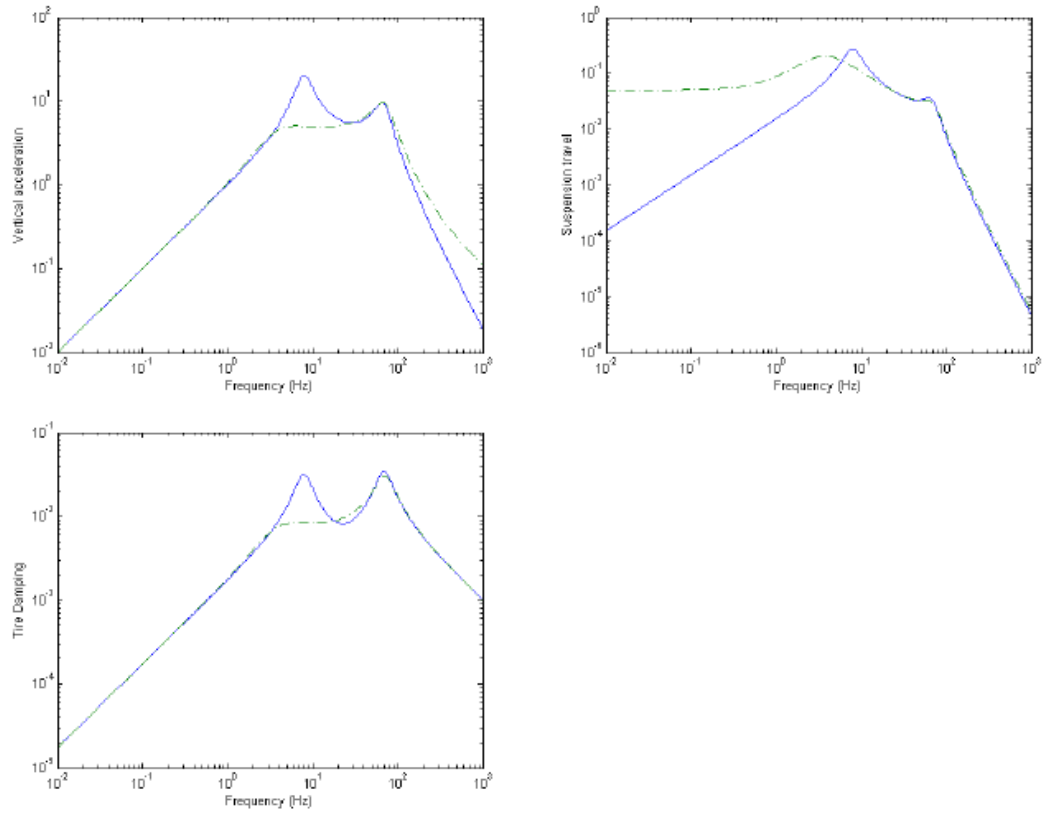


Figure 3.9 : The vertical acceleration, the suspension travel and the tire deflection frequency responses with $\alpha = 1$, $\mu = 1$ and $C_t = 50$ Ns/m; (—) passive suspension, (-.-) active suspension

Figure 3.10 shows the rms values of active and passive suspension systems when the tire damping is varied from 0 to 100 Ns/m for parameters $\alpha = 1$ and $\mu = 1$.

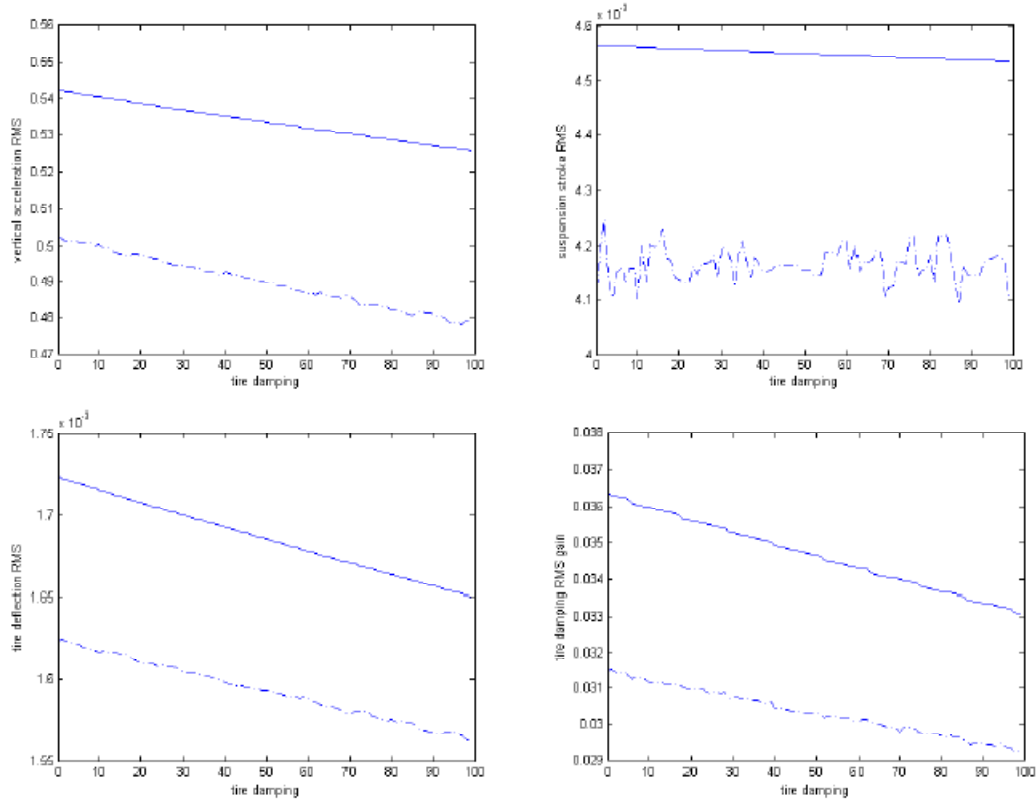


Figure 3.10 : The rms values and the tire deflection rms gain of the vehicle subjected to white noise velocity input as a function of C_t with $\alpha = 1$ and $\mu = 1$; (—) passive suspension, (-.-) active suspension

Effect of changes in the design parameters μ and α on the design problem was studied in the previous section. In this design, the response of the system was studied for only different values of ρ_1 . The rms vertical acceleration has been minimized when the rms suspension travel and the rms tire deflection have been kept below their upper bounds. The improvement on the rms vertical acceleration is around 8.22% in the third design. The rms values were calculated for different values of the design parameters μ and α they were shown on Table 3.7 and 3.8.

	The Closed-Loop Rms Values
The rms vertical acceleration	0.4015
The rms suspension travel	0.0044
The rms tire deflection	0.0018
The tire deflection rms gain	0.0429

Table 3.7 : The rms values of z_k , $k = 1,2,3$, and the tire deflection rms gain table of passive and active suspension systems with $\alpha = 1$, $\mu = 2$ and $C_t = 50$ Ns/m

	The Closed-Loop Rms Values
The rms vertical acceleration	0.4887
The rms suspension travel	0.0053
The rms tire deflection	0.0016
The tire deflection rms gain	0.0304

Table 3.8 : The rms values of z_k , $k = 1,2,3$, and the tire deflection rms gain table of passive and active suspension systems with $\alpha = 2$, $\mu = 1$ and $C_t = 50$ Ns/m

All these results claimed that, we can decrease the rms vertical acceleration when the rms suspension travel and the rms tire deflection were below the given bounds ν and γ respectively. Firstly, we changed only the rms tire deflection constraint limit. It did not have an influence on increasing the rms suspension travel above its upper limit. Likewise, when we changed only the upper limit of the rms suspension travel constraint, it did not have an effect on increasing the rms tire deflection above its maximum.

CHAPTER 4

CONCLUSIONS

In this thesis, we examined solutions of an quarter-car active suspension design problem with multiobjective output-feedback control via LMI synthesis. The problem was discussed for three cases. Some constraints were defined in all the three design examples. We also defined parameters for these constraints. For different parameter values, the response of the system was studied.

In the first design, we tried to minimize both the rms suspension travel and the rms vertical acceleration with the constraint on the rms tire damping. In the second and the third designs, we examined whether we can minimize only the rms vertical acceleration while the rms tire damping and the rms suspension travel below allowable maximum values. The results of all the three designs were given with the bode plots, the rms plots and the rms values.

As a result, in the first design, it was observed that the rms suspension travel can not be controlled when the rms vertical acceleration minimized. The other designs confirmed the expected behaviours on the rms values and plots. Namely, analysis and simulation result confirmed achieving better ride comfort while keeping suspension strokes within bounds and ensuring firm contact of the wheels to road.

4.1 Future Work

As a recommendation for the active suspension future work, we suggest using half-car and full-car models in the design. Especially full-car model gives us more realistic results. Also, multiobjective state-feedback again via LMI synthesis can be studied and responses can be examined.

In this thesis, the quarter-car model is parametrized for the white noise velocity road inputs. For the active suspension future work, we can use coloured noise velocity road inputs to parametrize the quarter-car model and to design active suspension.

This study can be used for productions of wheels and shock absorbers. And also, it can be examined usage of this method for the dynamical analysis of the vehicle (motor, clutch, gear box, etc.).

BIBLIOGRAPHY

- [1] Carsten Scherer, Pascal Gahinet, Mahmoud Chilali, “*Multiobjective Output Feedback Control via LMI Optimization*”, IEEE Transactions on Automatic Control, **42**(7), pages 896-911, July 1997
- [2] Pascal Gahinet, Arkadi Nemurovski, Alan J. Laub, Mahmoud Chilali, “*LMI Control Toolbox*”, May 1995
- [3] Hüseyin Akçay, Semiha Türkay, “*Influence Tire Damping on Multi Objective Control of Quarter-Car Active Suspensions*”, to appear in Proceedings of International Conference on Industrial Technology, Viña del Mar-Volparaiso Chile, March 2010
- [4] Hong Chen, Kong – Hui Guo, “*Constrained H_{∞} Control of Active Suspensions: An LMI Approach*”, IEEE Transactions on Control Systems Technology, **13**(3), pages 412-421, May 2005
- [5] Miaomiao Ma, Hong Chen, “*Constrained H_2 Control of Active Suspensions Using LMI Optimization*”, Proceedings of the 25th Chinese Control Conference, pages 702-707, August 2006
- [6] H. Chen, K. Guo, “*An LMI Approach to Multiobjective RMS Gain Control for Active Suspensions*”, Proceedings of the American Control Conference, pages 2646-2651, June 2001
- [7] Richard D. Braatz, Manfred Morari, “*On the Stability of Systems with Mixed Time-Varying Parameters*”, International Journal of Robust and Nonlinear Control, **7**, pages 105-112, 1997
- [8] Mohammed Chadli, Didier Maquin, José Ragot, “*An LMI Formulation for Output Feedback Stabilization in Multiple Model Approach*”, Proceedings of the 41st IEEE Conference on Decision and Control, pages 311-316, December 2002

- [9] Didier Henrion, Denis Arzelier, Dimitri Peaucella, Michael Sebek, “*An LMI Condition for Robust Stability of Polynomial Matrix Polytopes*”, *Automatica* **37**(2001), pages 461-468, September 2000
- [10] Vincent R. Marcopoli, Stephen M. Phillips, “*Analysis and Synthesis Tools for a Class of Actuator-Limited Multivariable Control Systems : A Linear Matrix Inequality Approach*”, *International Journal of Robust and Nonlinear Control*, **6**, pages 1045-1063, 1996
- [11] Carsten Scherer, Siep Weiland, “*Linear Matrix Inequality in Control*”, November 16, 2004
- [12] John Doyle, Bruce Francis, Allen Tannenbaum, “*Feedback Control Theory*”, Macmillan Publishing Co., 1990
- [13] David Banjerdpongchai, Jonathan P. How, “*Parametric Robust H_2 Control Design with Generalized Multipliers via LMI Synthesis*”, *International Journal of Control*, **70**(3), pages 481-503, 1998
- [14] Tae – Yong Doh, Kyoung Bog Jin, Myung Jin Chung, “*An LMI Approach to Iterative Learning Control for Uncertain Linear Systems*”, *ISIAC* 006.1-006.6, 1998
- [15] Yi Cao, Zhijia Yang, “*Multiobjective Process Controllability Analysis*”, *Computers and Chemical Engineering*, **28**(1-2), 15 January 2004
- [16] Kenzo Nonami, Selim Sivrioğlu, “*Active Vibration Control Using LMI – Based Mixed H_2/H_∞ State and Output Feedback Control with Nonlinearity*”, *Proceedings of 35th Conference on Decision and Control*, Japan, pages 161-166, December 1996
- [17] C. Poussot – Vassal, O. Sename, L. Dugard, P. Gaspar, Z. Szabo, J. Bokor, “*A New Semi – Active Suspension Control Strategy Through LPV Technique*”, *Control Engineering Practise* **16**(2008), pages 1519-1534, 2008

- [18] K. Galkowski, J. Lam, E. Rogers, S. Xu, B. Sulikowski, W. Paszke, D. H. Owens, “*LMI Based Stability Analysis and Robust Controller Design for Discrete Linear Repetitive Processes*”, International Journal of Robust and Nonlinear Control, **13**, pages 1195-1211, 2003
- [19] Stephen Boyd, “*Robust Control Tools: Graphical User – Interfaces and LMI Algorithms*”, Systems, Control and Information, **38**(3), pages 111-117, March 1994
- [20] Carsten W. Scherer, “*An Efficient Solution to Multi - Objective Control Problems with LMI Objectives*”, Systems and Control Letters **40**(2000), pages 43-57, 4 December 1999
- [21] George Z. Angelis, “*System Analysis, Modelling and Control with Polytopic Linear Models*”, Eindhoven University, 2001
- [22] Stephen Boyd, Laurent El Ghaoui, Eric Feron, Venkataramanan Balakrishnan, “*Linear Matrix Inequalities in System and Control Theory*”, SIAM Studies in Applied Mathematics, 1994
- [23] A. Megretski, “*Multivariable Control Systems*”, Massachusetts Institute of Technology, Version of March 29, 2004
- [24] Emmet J. Ientilucci, “*Using Singular Value Decomposition*”, Rochester Institute of Technology, May 29, 2003
- [25] Murat Akın, Leyla Gören, “*Dinamik Durum Geribeslemesi ile Ayrık H_{∞} Model Eşleme Problemi*”, ITU Dergisi, **3**(6), pages 25-32, December 2004
- [26] Neculai Andrei, “*Modern Control Theory*”, Research Institute for Informatics, Center for Advanced Modeling and Optimization
- [27] Semiha Türkay, Hüseyin Akçay, “*A Study of Random Vibration Characteristics of the Quarter-Car Model*”, Journal of Sound and Vibration, **282**(2005), pages 111-124, 2005
- [28] Hamid D. Taghirad, E. Esmailzadeh, “*Automobile Passenger Comfort Assured Through LQG/LQR Active Suspension*”, Journal of Vibration and Control, **4**(5), pages 603-618, 1998

- [29] Izumi Masubuchi, Atsumi Ohara, Nobuhide Suda, “*LMI-Based Controller Synthesis: a Unified Formulation and Solution*”, International Journal of Robust and Nonlinear Control **8**, pages 669-686, 1998
- [30] <http://mathworld.wolfram.com/MatrixTrace.html>, 1994 – 2009 The MathWorks, Inc.

Appendix A

```

%QUARTER CAR ACTIVE SUSPENSION SYSTEM DESIGN%
%LMI Hinfinity/H2%
%ASLI SOYİÇ - 36019402702 %

%VALUES OF VARIABLES%
ms = 240; mu = 36; Cs = 980; ks = 16000; kt = 160000;

v = 20; % vehicle velocity

n0 = 0.15708;
kappa = 0.76e-5;
K_n = 2*pi*n0*sqrt(kappa*v);

% 0 <= Ct <= 100 %
for i = 1:100,
    Ct = i-1;
    damping(i,1) = Ct;

% dx/dt= A*x + B1*w + B2*u %
A = [0 0 1 -1;0 0 0 1;-(ks/ms) 0 -(Cs/ms) (Cs/ms);(ks/mu) -(kt/mu)
(Cs/mu) -((Cs+Ct)/mu)];
B1 = [0;-1;0;(Ct/mu)];
B2 = [0;0;-(1/ms);(1/mu)];

%tire deflection z_i = C_i*x + D1i*Vi + D2i*u %

C_i = [0 1 0 0];
D1i = 0; D2i=0;

%z_2 = C2*x + D12*Vi + D22*u %

C2 = [-(ks/ms) 0 -(Cs/ms) (Cs/ms);1 0 0 0];
D12 = [0;0];
D22 = [-(1/ms);0];

% exogenous output z = Cz*x + D1z*Vi + D2z*u %

Cz = [-(ks/ms) 0 -(Cs/ms) (Cs/ms);1 0 0 0;0 1 0 0];
D1z = [0;0;0];
D2z = [-(1/ms);0;0];

%measurement output y = C_y*x + D1y*Vi + D2y*u%
Cy = [-(ks/ms) 0 -(Cs/ms) (Cs/ms);1 0 0 0];
D1y = [0;0];
D2y = [-(1/ms);0];

%RMS values of system%

n_i = normhinf(A,B1,C_i,D1i); %H_inf norm of tire deflection%
n_iop(i,1) = n_i;

```



```

n_1 = norm2(ltisys(A,B1,C2(1,:),D12(1,:)));
    %H2 norm of vertical acceleration%
n_2 = norm2(ltisys(A,B1,C2(2,:),D12(2,:)));
    %H2 norm of suspension travel%
n_3 = norm2(ltisys(A,B1,C_i,D1i));
    %H2 norm of tire deflection%
n1_op(i,1) = K_n*n_1;
n2_op(i,1) = K_n*n_2;
n3_op(i,1) = K_n*n_3;

%multiobjective control design%

Tz = diag([1/n_1 1/n_2]);
lamda = 0.1;
W = [1 0;0 lamda]*Tz;    %scaling factor%

sys = ltisys(A,[B1 B2],[C_i;W*C2;Cy],[D1i D2i;W*D12 W*D22;D1y
D2y]);
beta = 1;

[gopt,h2opt,K] = hinfmix(sys,[2 2 1],[beta*n_i 0 0 1]);

%K is the output feedback controller %
%state space equations of controller%

[Ak,Bk,Ck,Dk] = ltiss(K);

%CLOSED LOOP STATE SPACES MATRICES%

M = inv(1-(Dk*D2y));
A_cl = [A+B2*M*Dk*Cy B2*M*Ck;Bk*(Cy+D2y*M*Dk*Cy) Ak+Bk*D2y*M*Ck];
B_cl = [(B1+B2*M*Dk*D1y);Bk*(D1y+D2y*M*Dk*D1y)];
C_cl = [(Cz+D2z*M*Dk*Cy) D2z*M*Ck];
D_cl = [D1z+D2z*M*Dk*D1y];

%CLOSED LOOP RMS VALUES%

n_icl(i,1) = normhinf(A_cl,B_cl,C_cl(3,:),D_cl(3,:));
n1_cl(i,1) = K_n*norm2(ltisys(A_cl,B_cl,C_cl(1,:),D_cl(1,:)));
n2_cl(i,1) = K_n*norm2(ltisys(A_cl,B_cl,C_cl(2,:),D_cl(2,:)));
n3_cl(i,1) = K_n*norm2(ltisys(A_cl,B_cl,C_cl(3,:),D_cl(3,:)));

end

figure(1)
plot(damping,n1_op,damping,n1_cl,'b-.')
ylabel('RMS vertical acceleration ');
xlabel('tire damping');

figure(2)
plot(damping,n2_op,damping,n2_cl,'b-.');
ylabel('RMS suspension stroke');
xlabel('tire damping');

```

```

figure(3)
plot(damping,n3_op,damping,n3_cl,'b-.');
ylabel('RMS tire deflection');
xlabel('tire damping');

figure(4)
plot(damping,n_iop,damping,n_icl,'b-.');
ylabel('tire deflection RMS gain');
xlabel('tire damping');

% BODE PLOTS %

sys_open = ss(A,B1,Cz,D1z);
sys_cls = ss(A_cl,B_cl,C_cl,D_cl);

w = logspace(-2,3,1000);
sys_openg = frd(sys_open,w);
sys_clsg = frd(sys_cls,w);

figure(5)
loglog(abs(sys_openg(1,:)),abs(sys_clsg(1:)), '-. ');
xlabel('Frequency (Hz)');
ylabel('Vertical acceleration');

figure(6)
loglog(abs(sys_openg(2,:)),abs(sys_clsg(2:)), '-. ');
xlabel('Frequency (Hz)');
ylabel('Suspension travel');

figure(7)
loglog(abs(sys_openg(3,:)),abs(sys_clsg(3:)), '-. ');
xlabel('Frequency (Hz)');
ylabel('Tire Damping');

```

Appendix B

```

% LMI CONTROL IN ACTIVE SUSPENSION
% ASLI SOYIÇ - 36019402702

ms=240; mu=36; Cs=980; ks=16000; kt=160000;

v=20; % vehicle velocity m/s

n0=0.15708;
kappa=0.76e-5;
K_n=2*pi*n0*sqrt(kappa*v);

%%% 0 <= Ct <= 100 %%%

for i=1:100,
    Ct=i-1;
    damping(i,1)=Ct;

    %%% dx/dt= A*x + B1*Vi + B2*u %%%
    A = [0 0 1 -1;0 0 0 1;-(ks/ms) 0 -(Cs/ms) (Cs/ms);(ks/mu) -(kt/mu)
        (Cs/mu) -((Cs+Ct)/mu)];
    B1 = [0;-1;0;(Ct/mu)];
    B2 = [0;0;-(1/ms);(1/mu)];

    %%% z = Cz*x + Dzw*Vi + Dzu*u %%%
    Cz = [-(ks/ms) 0 -(Cs/ms) (Cs/ms);1 0 0 0;0 1 0 0];
    Dzw = [0;0;0];
    Dzu = [-(1/ms);0;0];

    %%% y = C*x + Dy*u %%%
    C = [-(ks/ms) 0 -(Cs/ms) (Cs/ms)];
    Dy = [-(1/ms)];
    D1y = [0];

    %%% H_infinity Z_i = C_i*x + D11*Vi + D12*u - tire deflection
    %%%
    C_i = [0 1 0 0];
    D11 = 0;
    D12 = 0;

    % output for H_2 z_2 = C2*x + D21*Vi + D22*u - suspension %
    C2 = [-(ks/ms) 0 -(Cs/ms) (Cs/ms);1 0 0 0];
    D21 = [0;0];
    D22 = [-(1/ms);0];

    %H_inf norm of tire deflection%
    n_i=normhinf(A,B1,C_i,D11);
    n_iop(i,1)=n_i;

    %%% AÇIK DÖNGÜ RMS DEĞERLERİ %%%
    n1=norm2(ltisys(A,B1,Cz(1,:),Dzw(1,:)));
    n2=norm2(ltisys(A,B1,Cz(2,:),Dzw(2,:)));
    n_3=norm2(ltisys(A,B1,Cz(3,:),Dzw(3,:)));
    n1_op(i,1)=K_n*n1;

```

```

n2_op(i,1)=K_n*n2;
n3_op(i,1)=K_n*n_3;

Tz=diag([1/n1 1]);
lamda=1;
W=[1 0;0 lamda]*Tz;      %scaling factor%
C_2 = W*C2;
D_21 = W*D21;
D_22 = W*D22;

%%%% LMI VARIABLES %%%%
setlmis([]);

X = lmivar(1,[4 1]);
Y = lmivar(1,[4 1]);
A_tilda = lmivar(2,[4 4]);
B_tilda = lmivar(2,[4 1]);
C_tilda = lmivar(2,[1 4]);
Dk = lmivar(2,[1 1]);      % Dk = D_tilda
[Q,n,Q1] = lmivar(1,[2 1]);
gamma = lmivar(2,[1 1]);

%%%% LMI CONSTRAINTS %%%%
%%%% H_inf PERFORMANCE %%%%

lmiterm([1 1 1 X],A,1,'s');      %LMI #1 : X*A' + A*X
lmiterm([1 1 1 C_tilda],B2,1,'s');
% LMI #1 : B2*C_tilda + C_tilda'*B2'

lmiterm([1 2 1 A_tilda],1,      % LMI #1 : A_tilda
[1 2 1 0],A');                % LMI #1 : A'
lmiterm([1 2 1 -Dk],C',(inv(1-Dk*Dy))'*B2');
% LMI #1 : ( B2*inv(1-Dk*Dy)*D_tilda*C )'

lmiterm([1 2 2 Y],1,A,'s');
% LMI #1 : Y*A + A'*Y'
lmiterm([1 2 2 B_tilda],1,C,'s');
% LMI #1 : B_tilda*C + C'*B_tilda'

lmiterm([1 3 1 0],B1');      % LMI #1 : B1'

lmiterm([1 3 2 -Y],B1',1      % LMI #1 : B1'*Y'

lmiterm([1 3 3 0],-1);      % LMI #1 : -gamma*I

lmiterm([1 4 1 X],C_i,1);      % LMI #1 : C_i*X
lmiterm([1 4 1 C_tilda],D12,1); % LMI #1 : D12*C_tilda

lmiterm([1 4 2 0],C_i);      % LMI #1 : C_i
lmiterm([1 4 2 Dk],D12*inv(1-Dk*Dy),C);
% LMI #1 : D12*inv(1-Dk*Dy)*Dk*C

lmiterm([1 4 3 0],D11);      % LMI #1 : D11

lmiterm([1 4 4 gamma],-1,1); % LMI #1 : -gamma*I

```

```

%% H_2 PERFORMANCE

lmiterm([-2 1 1 Q],1,1); % LMI #2 : Q

lmiterm([-2 1 2 X],C_2,1); % LMI #2 : C_2*X

lmiterm([-2 1 2 C_tilda],D_22,1); % LMI #2 : D22*C_tilda

lmiterm([-2 1 3 0],C_2); % LMI #2 : C_2
lmiterm([-2 1 3 Dk],D_22*inv(1-Dk*Dy),C);
% LMI #2 : D22*inv(1-Dk*Dy)*Dk*C

lmiterm([-2 2 2 X],1,1); % LMI #2 : X

lmiterm([-2 2 3 0],1); % LMI #2 : I

lmiterm([-2 3 3 Y],1,1); % LMI #2 : Y

%% trace(Q) < nu
qdec = lmivar(3,diag(Q1));
lmiterm([3 1 1 trace(qdec)],ones(1,2),0.5,'s');
% LMI #3 : trace(Q)
lmiterm([3 1 1 qdec],[-1 0],0.5,'s');
lmiterm([3 1 1 0],[-(n2^2)]; % LMI #3 : nu
sclf=max(1,nu0^2/1e3);

%% P > 0

lmiterm([-4 1 1 X],1,1); % LMI #4 : X

lmiterm([-4 2 1 0],1); % LMI #4 : I

lmiterm([-4 2 2 Y],1,1); % LMI #4 : Y

%% gamma < n_i^2

lmiterm([5 1 1 gamma],1,1); % LMI #5 : gamma
lmiterm([-5 1 1 0],[n_i^2]); % LMI #5 : n_i^2

%% Q > 0

lmiterm([-6 1 1 Q],1,1);

lmisys = getlmis;

n_dec = decnbr(lmisys); % number of decision variables %
c = zeros(n_dec,1); % dimensions 'c' c'*x%

for j=1:n_dec, % objective function definition %

    qj = defcx(lmisys,j,qdec);
    c(j) = sqrt(trace(qj(1,1)));

end

```

```

options = [0 200 1e8 0 0];
[copt,xopt] = mincx(lmisys,c',options);

%%%% VALUES OF LMI VARIABLES %%%%

X = dec2mat(lmisys,xopt,X);
Y = dec2mat(lmisys,xopt,Y);
A_tilda = dec2mat(lmisys,xopt,A_tilda);
B_tilda = dec2mat(lmisys,xopt,B_tilda);
C_tilda = dec2mat(lmisys,xopt,C_tilda);
Dk = dec2mat(lmisys,xopt,Dk);
Q = dec2mat(lmisys,xopt,Q);
gamma = dec2mat(lmisys,xopt,gamma);

[u,sd,v]=svd(eye(4)-X*Y);           %M*N' = I - X*Y
N=v;  M=u*sd;

%%%% PARAMETERS OF CONTROLLER %%%%

Ck = (1-Dk*Dy)*C_tilda*transpose(inv(M))-Dk*C*X*transpose(inv(M));
Bk = inv(N)*(B_tilda-Y'*B2*inv(1-Dk*Dy)*Dk)
      *inv(1+Dy*inv(1-Dk*Dy)*Dk);
Ak = inv(N)*(A_tilda-(Y'*A*X)-(Y'*B2*inv(1-Dk*Dy)*Dk*C*X)
      -(Y'*B2*inv(1-Dk*Dy)*Ck*M')-(N*Bk*C*X)
      -(N*Bk*Dy*inv(1-Dk*Dy)*Dk*C*X)
      -(N*Bk*Dy*inv(1-Dk*Dy)*Ck*M'))*inv(M');

%%%% CLOSED-LOOP SYSTEM %%%%

F = inv(1-(Dk*Dy));
A_cl = [A+B2*F*Dk*C B2*F*Ck;Bk*(C+Dy*F*Dk*C) Ak+Bk*Dy*F*Ck];
B_cl = [(B1+B2*F*Dk*D1y);Bk*(D1y+Dy*F*Dk*D1y)];
C_cl = [(Cz+Dzu*F*Dk*C) Dzu*F*Ck];
D_cl = [Dzw+Dzu*F*Dk*D1y];

n_icl(i,1) = normhinf(A_cl,B_cl,C_cl(3,:),D_cl(3,:));
n1_cl(i,1) = K_n*norm2(ltisys(A_cl,B_cl,C_cl(1,:),D_cl(1,:)));
n2_cl(i,1) = K_n*norm2(ltisys(A_cl,B_cl,C_cl(2,:),D_cl(2,:)));
n3_cl(i,1) = K_n*norm2(ltisys(A_cl,B_cl,C_cl(3,:),D_cl(3,:)));

end

sys_open = ss(A,B1,Cz,Dzw);
sys_cls = ss(A_cl,B_cl,C_cl,D_cl);

w = logspace(-2,3,1000);
sys_openg = frd(sys_open,w);
sys_clsg = frd(sys_cls,w);

figure(1)
loglog(abs(sys_openg(1,:)),abs(sys_clsg(1:,:)),'-');
xlabel('Frequency (Hz)');
ylabel('Vertical acceleration');

figure(2)
loglog(abs(sys_openg(2,:)),abs(sys_clsg(2:,:)),'-');
xlabel('Frequency (Hz)');
ylabel('Suspension travel');

```

```

figure(3)
loglog(abs(sys_openg(3,:)),abs(sys_clsg(3,:)),'-.');
xlabel('Frequency (Hz)');
ylabel('Tire Damping');

figure(4)
plot(damping,n1_op,damping,n1_cl,'b-.')
ylabel('vertical acceleration RMS');
xlabel('tire damping');

figure(5)
plot(damping,n2_op,damping,n2_cl,'b-.');
ylabel('suspension stroke RMS');
xlabel('tire damping');

figure(6)
plot(damping,n3_op,damping,n3_cl,'b-.');
ylabel('tire deflection RMS');
xlabel('tire damping');

figure(7)
plot(damping,n_iop,damping,n_icl,'b-.');
ylabel('tire damping RMS gain');
xlabel('tire damping');

```

Appendix C

```

% LMI CONTROL IN ACTIVE SUSPENSION
% ASLI SOYIÇ - 36019402702

ms=240; mu=36; Cs=980; ks=16000; kt=160000;

v=20; % vehicle velocity

n0=0.15708;
kappa=0.76e-5;
K_n=2*pi*n0*sqrt(kappa*v);

%%% 0 <= Ct <= 100 %%%

for i=1:100,
    Ct=i-1;
    damping(i,1)=Ct;

%%% dx/dt= A*x + B1*Vi + B2*u %%%

A = [0 0 1 -1;0 0 0 1;-(ks/ms) 0 -(Cs/ms) (Cs/ms); (ks/mu) -(kt/mu)
(Cs/mu) -((Cs+Ct)/mu)];
B1 = [0;-1;0; (Ct/mu)];
B2 = [0;0;-(1/ms); (1/mu)];

%%% z = Cz*x + Dzw*Vi + Dzu*u %%%

Cz = [-(ks/ms) 0 -(Cs/ms) (Cs/ms);1 0 0 0;0 1 0 0];
Dzw = [0;0;0];
Dzu = [-(1/ms);0;0];

%%% y = C*x + Dy*u %%%

C = [-(ks/ms) 0 -(Cs/ms) (Cs/ms)];
Dy = [-(1/ms)];
D1y = [0];

%%% H_inf Z_i = C_i*x + D11*Vi + D12*u - tire deflection %%%

C_i = [0 1 0 0];
D11 = 0;
D12 = 0;

% output for H_2 z_2 = C2*x + D21*Vi + D22*u - suspension %

C2 = [-(ks/ms) 0 -(Cs/ms) (Cs/ms);1 0 0 0];
D21 = [0;0];
D22 = [-(1/ms);0];

n_i=normhinf(A,B1,C_i,D11);
%H_inf norm of tire deflection%
n_iop(i,1)=n_i;

```



```

%%%% OPEN-LOOP RMS VALUES %%%

n1=norm2(ltisys(A,B1,Cz(1,:),Dzw(1,:)));
%H2 norm of vertical acceleration%
n2=norm2(ltisys(A,B1,Cz(2,:),Dzw(2,:)));
%H2 norm of suspension travel%
n3=norm2(ltisys(A,B1,Cz(3,:),Dzw(3,:)));
%H2 norm of tire deflection%
n1_op(i,1)=K_n*n1;
n2_op(i,1)=K_n*n2;
n3_op(i,1)=K_n*n3;

%%%% LMI DEĞİŞKENLERİ %%%
C_2=C2;
D_21=D21;
D_22=D22;

%%%% LMI CONSTRAINTS %%%

setlmis([]);

X = lmivar(1,[4 1]);
Y = lmivar(1,[4 1]);
A_tilda = lmivar(2,[4 4]);
B_tilda = lmivar(2,[4 1]);
C_tilda = lmivar(2,[1 4]);
Dk = lmivar(2,[1 1]);           % Dk = D_tilda
[Q,n,Q1] = lmivar(1,[2 1]);
gamma = lmivar(2,[1 1]);

%%%% H_inf PERFORMANCE %%%

lmiterm([1 1 1 X],A,1,'s');           %LMI #1 : X*A' + A*X
lmiterm([1 1 1 C_tilda],B2,1,'s');
% LMI #1 : B2*C_tilda + C_tilda'*B2'

lmiterm([1 2 1 A_tilda],1,1);         % LMI #1 : A_tilda
lmiterm([1 2 1 0],A');                % LMI #1 : A'
lmiterm([1 2 1 -Dk],C',(inv(1-Dk*Dy))'*B2');
% LMI #1 : ( B2*inv(1-Dk*Dy)*D_tilda*C )'

lmiterm([1 2 2 Y],1,A,'s');
% LMI #1 : Y*A + A'*Y'
lmiterm([1 2 2 B_tilda],1,C,'s');
% LMI #1 : B_tilda*C + C'*B_tilda'

lmiterm([1 3 1 0],B1');               % LMI #1 : B1'

lmiterm([1 3 2 -Y],B1',1);           % LMI #1 : B1'*Y'

lmiterm([1 3 3 0],-1);               % LMI #1 : -gamma*I

lmiterm([1 4 1 X],C_i,1);            % LMI #1 : C_i*X
lmiterm([1 4 1 C_tilda],D12,1);     % LMI #1 : D12*C_tilda

lmiterm([1 4 2 0],C_i);              % LMI #1 : C_i
lmiterm([1 4 2 Dk],D12*inv(1-Dk*Dy),C);

```

```

% LMI #1 : D12*inv(1-Dk*Dy)*Dk*C

lmiterm([1 4 3 0],D11); % LMI #1 : D11

lmiterm([1 4 4 gamma],[-1,1]); % LMI #1 : -gamma*I

%%%% H_2 PERFORMANCE %%%%

lmiterm([-2 1 1 Q],1,1); % LMI #2 : Q

lmiterm([-2 1 2 X],C_2,1); % LMI #2 : C_2*X

lmiterm([-2 1 2 C_tilda],D_22,1); % LMI #2 : D22*C_tilda

lmiterm([-2 1 3 0],C_2);
% LMI #2 : C_2
lmiterm([-2 1 3 Dk],D_22*inv(1-Dk*Dy),C);
% LMI #2 : D22*inv(1-Dk*Dy)*Dk*C

lmiterm([-2 2 2 X],1,1); % LMI #2 : X

lmiterm([-2 2 3 0],1); % LMI #2 : I

lmiterm([-2 3 3 Y],1,1); % LMI #2 : Y

%%%% trace(Q) < nu %%%%

qdec = lmivar(3,diag(Q1));
lmiterm([3 1 1 trace(qdec)],ones(1,2),0.5,'s');
% LMI #3 : trace(Q)
lmiterm([3 1 1 qdec],[-1 0],1/2,'s');
lmiterm([3 1 1 0],[-((n2)^2)]; % LMI #3 : nu

%%%% P > 0 %%%%

lmiterm([-4 1 1 X],1,1); % LMI #4 : X

lmiterm([-4 2 1 0],1); % LMI #4 : I

lmiterm([-4 2 2 Y],1,1); % LMI #4 : Y

%%%% gamma < n_i^2 %%%%

lmiterm([5 1 1 gamma],1,1); % LMI #5 : gamma
lmiterm([-5 1 1 0],[n_i^2]); % LMI #5 : n_i^2

%%%% Q > 0 %%%%

lmiterm([-6 1 1 Q],1,1);

lmisys = getlmis;

n_dec = decnbr(lmisys); % number of decision variables %
c = zeros(n_dec,1); % dimensions 'c' c'*x%

```

```

for j=1:n_dec, % objective function definition %

    qj = defcx(lmisys,j,qdec);
    c(j) = sqrt(trace(qj(1,1)));

end

options = [0 0 0 0 0];
[copt,xopt] = mincx(lmisys,c',options);

%%% VALUES OF LMI VARIABLES %%%

X = dec2mat(lmisys,xopt,X);
Y = dec2mat(lmisys,xopt,Y);
A_tilda = dec2mat(lmisys,xopt,A_tilda);
B_tilda = dec2mat(lmisys,xopt,B_tilda);
C_tilda = dec2mat(lmisys,xopt,C_tilda);
Dk = dec2mat(lmisys,xopt,Dk);
Q = dec2mat(lmisys,xopt,Q);
gamma = dec2mat(lmisys,xopt,gamma);

[u,sd,v]=svd(eye(4)-X*Y); %M*N' = I - X*Y
N=v; M=u*sd;

%%% PARAMETERS OF CONTROLLER %%%

Ck = (1-Dk*Dy)*C_tilda*transpose(inv(M))-Dk*C*X*transpose(inv(M));
Bk = inv(N)*(B_tilda-Y'*B2*inv(1-Dk*Dy)*Dk)
    *inv(1+Dy*inv(1-Dk*Dy)*Dk);
Ak = inv(N)*(A_tilda-(Y'*A*X)-(Y'*B2*inv(1-Dk*Dy)*Dk*C*X)
    -(Y'*B2*inv(1-Dk*Dy)*Ck*M')-(N*Bk*C*X)
    -(N*Bk*Dy*inv(1-Dk*Dy)*Dk*C*X)
    -(N*Bk*Dy*inv(1-Dk*Dy)*Ck*M'))*inv(M');

%%% CLOSED-LOOP SYSTEM %%%

F = inv(1-(Dk*Dy));
A_cl = [A+B2*F*Dk*C B2*F*Ck;Bk*(C+Dy*F*Dk*C) Ak+Bk*Dy*F*Ck];
B_cl = [(B1+B2*F*Dk*D1y);Bk*(D1y+Dy*F*Dk*D1y)];
C_cl = [(Cz+Dzu*F*Dk*C) Dzu*F*Ck];
D_cl = [Dzw+Dzu*F*Dk*D1y];

n_icl(i,1) = normhinf(A_cl,B_cl,C_cl(3,:),D_cl(3,:));
n1_cl(i,1) = K_n*norm2(ltisys(A_cl,B_cl,C_cl(1,:),D_cl(1,:)));
n2_cl(i,1) = K_n*norm2(ltisys(A_cl,B_cl,C_cl(2,:),D_cl(2,:)));
n3_cl(i,1) = K_n*norm2(ltisys(A_cl,B_cl,C_cl(3,:),D_cl(3,:)));

end

sys_open = ss(A,B1,Cz,Dzw);
sys_cls = ss(A_cl,B_cl,C_cl,D_cl);

w = logspace(-2,3,1000);
sys_openg = frd(sys_open,w);
sys_cls_g = frd(sys_cls,w);

```

```

figure(1)
loglog(abs(sys_openg(1,:)),abs(sys_cls(1,:)),'-.');
xlabel('Frequency (Hz)');
ylabel('Vertical acceleration');

figure(2)
loglog(abs(sys_openg(2,:)),abs(sys_cls(2,:)),'-.');
xlabel('Frequency (Hz)');
ylabel('Suspension travel');

figure(3)
loglog(abs(sys_openg(3,:)),abs(sys_cls(3,:)),'-.');
xlabel('Frequency (Hz)');
ylabel('Tire Damping');

figure(4)
plot(damping,n1_op,damping,n1_cl,'b-.');
ylabel('vertical acceleration RMS');
xlabel('tire damping');

figure(5)
plot(damping,n2_op,damping,n2_cl,'b-.');
ylabel('suspension stroke RMS');
xlabel('tire damping');

figure(6)
plot(damping,n3_op,damping,n3_cl,'b-.');
ylabel('tire deflection RMS');
xlabel('tire damping');

figure(7)
plot(damping,n_iop,damping,n_icl,'b-.');
ylabel('tire damping RMS gain');
xlabel('tire damping');

```